Irfu - CEA Saclay
Institut de recherche sur les lois fondamentales de l'Univers

l'Observatoire de Paris — LESIA

Exploration des ceintures de radiations aux basses fréquences avec LOFAR

J. N. Girard*, P. Zarka, C. Tasse, S. Hess,
I. de Pater, B. Cecconi, D. Santos-Costa, R. Sault, R. Strom, R. Courtin
M. Hofstadter, N. Nettelmann, A. Sicard-Piet, L. Lorenzato, R. Fende
and the LOFAR Planets-exoplanets Working Group

*AIM/Irfu/SAp, CEA Saclay, France

LabEx UnivEarthS

université PARIS DIDEROT PARIS 7

Jupiter

- Giant magnetized gaseous planet in fast rotation (P ~ 10h)

$B_{eq}(L=1)$ ~ 4.3 G

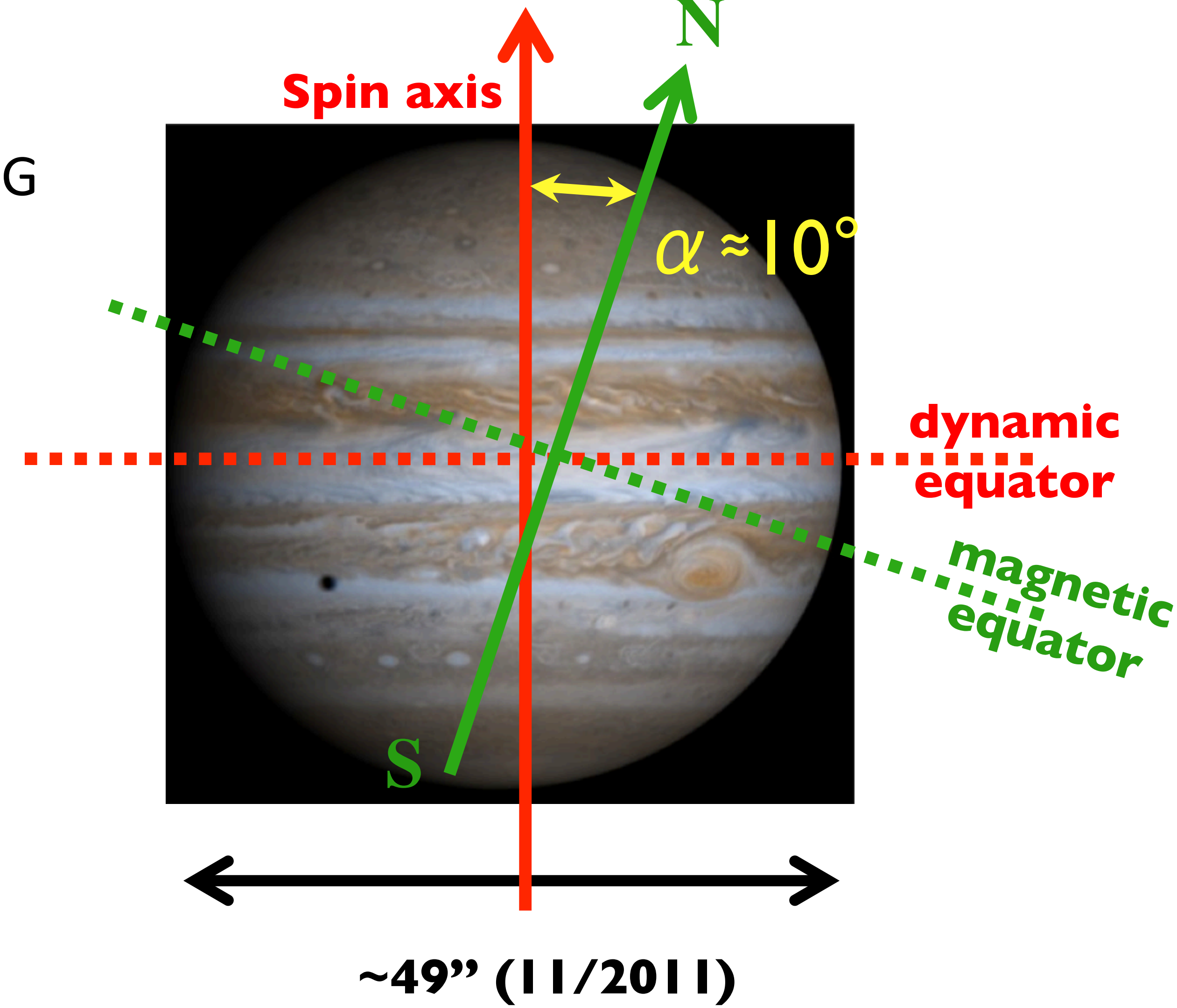

- « System III » coordinate system (1965) - $P_{Jupiter}$ = 9 h 55 m 29 s

The various radio emissions at Jupiter

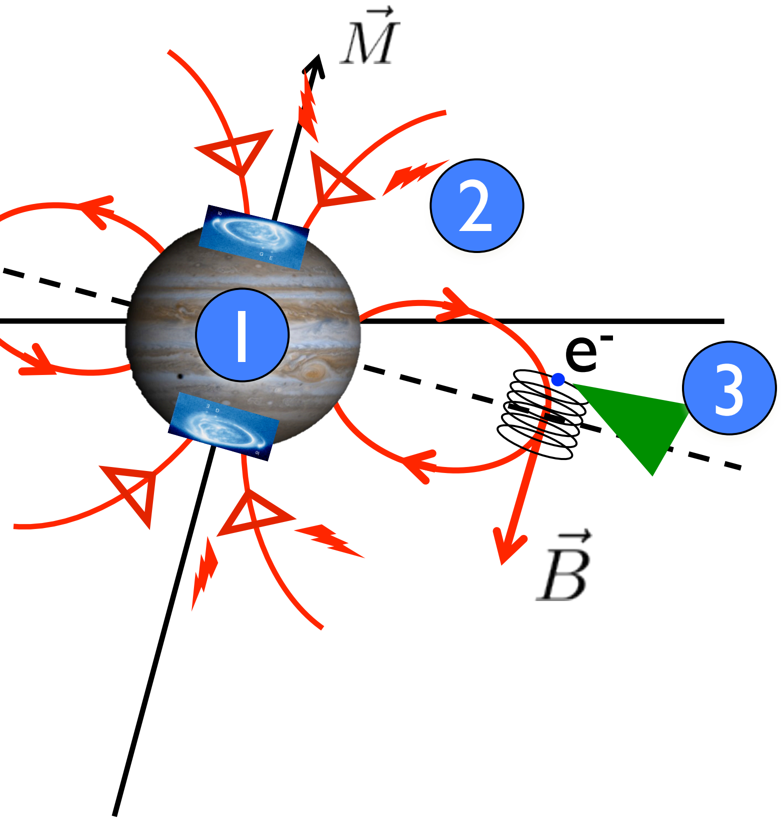

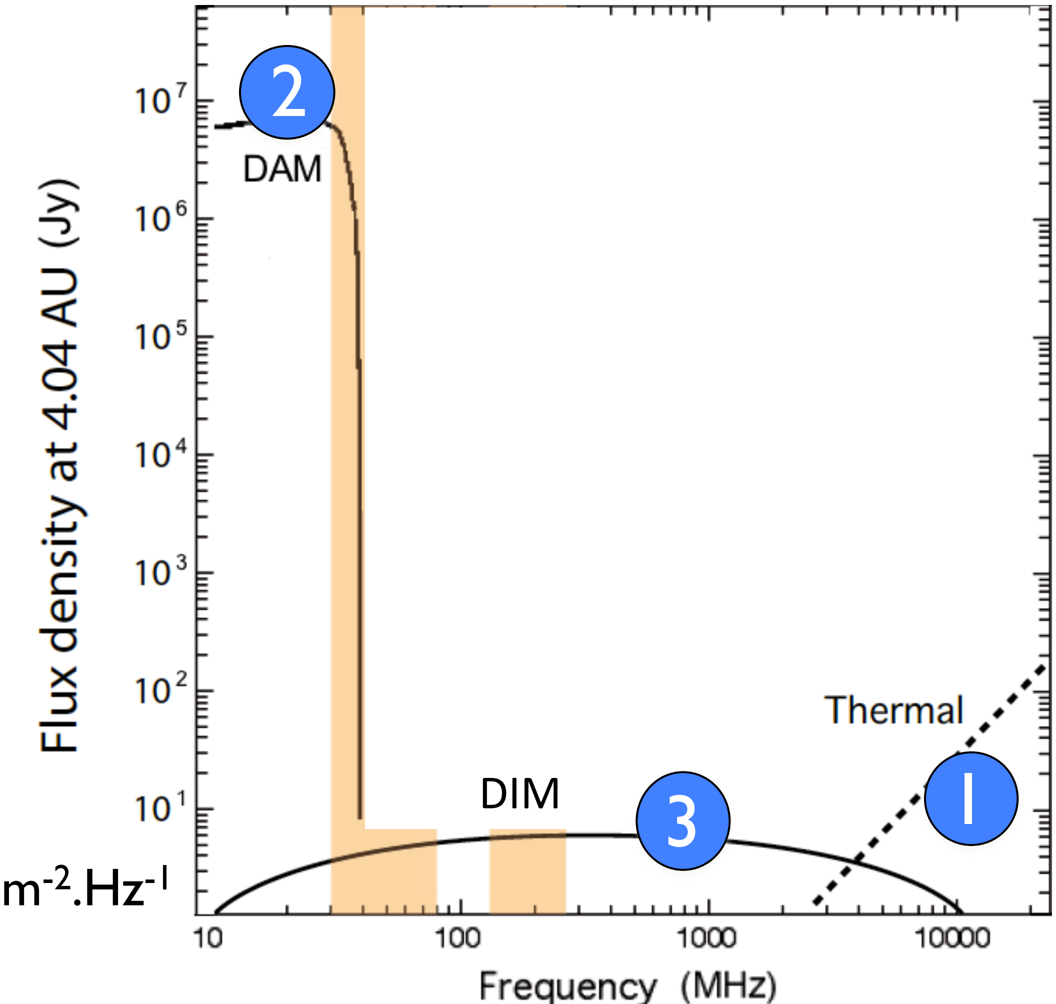

1 Jy = 10^{-26} W.m^{-2}.Hz^{-1}

1 **Thermal emission** (λ ~ cm)

2 **Cyclotron emission** (λ ≥ Dm)

3 **Synchrotron emission from radiation belts** (λ = cm-dm-m)

Properties of the radiation belt radio emission

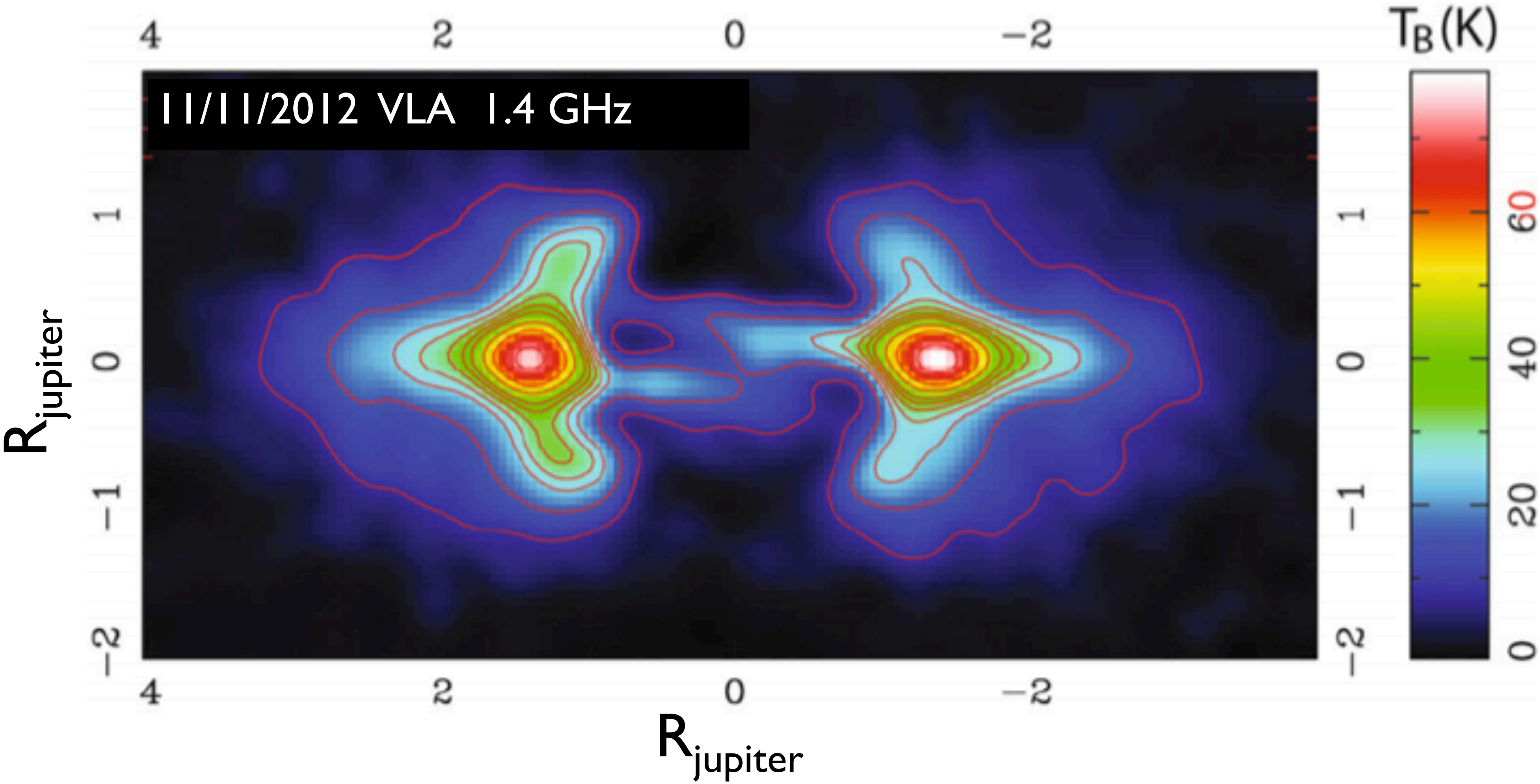

- Relativistic electrons (100s keV → 100s MeV) trapped near the magnetic equator
- Optically thin medium → Max of emission on both planet sides
- Anisotropic (beamed) and polarized emissions (~20-25% linearly, <1% circularly)
- Brightness distribution → interaction between e^- and inner satellites/dust ring…

Past observations

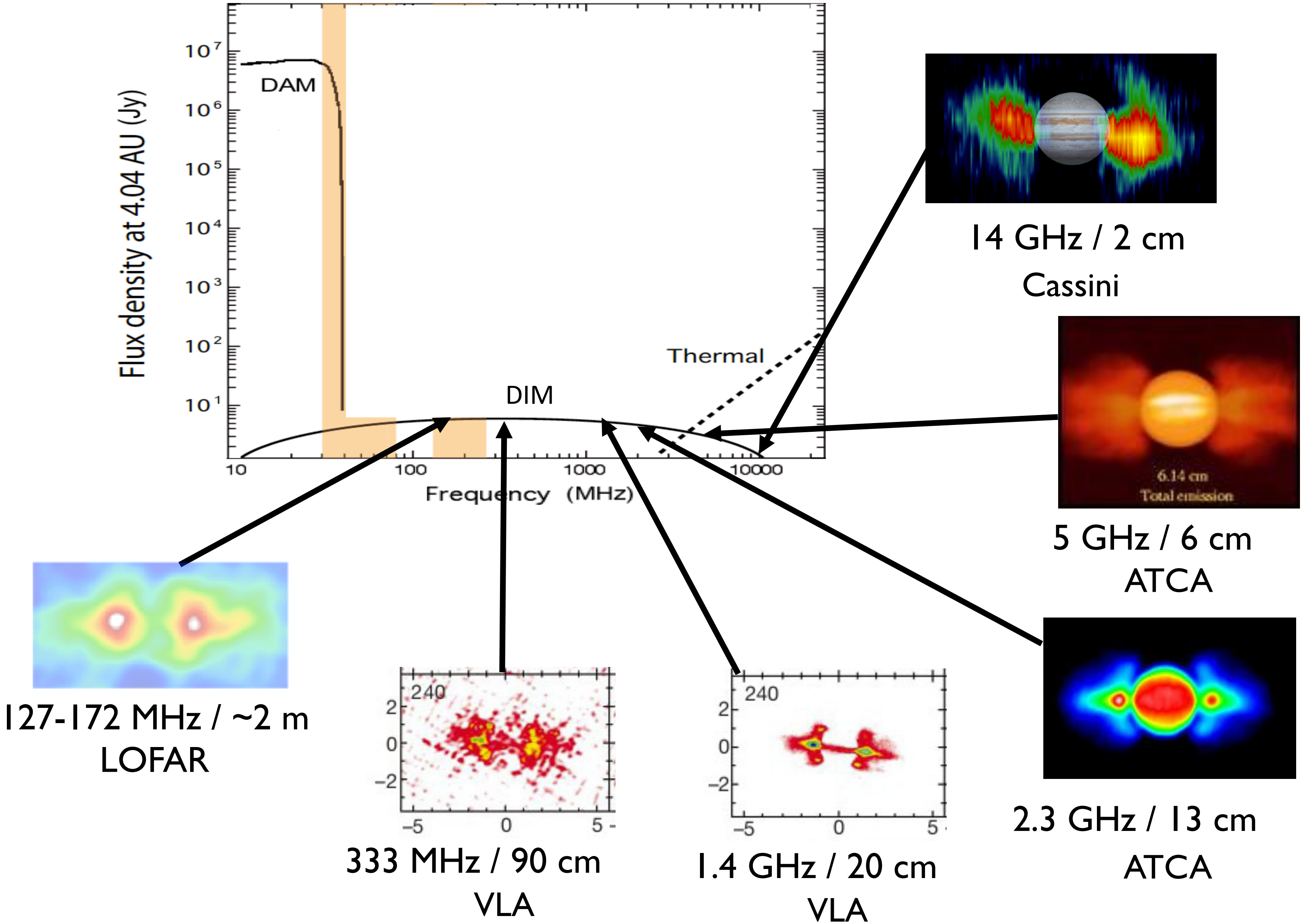

- Low frequencies → electrons with lower energies / lower |B| regions $\nu_{max} \propto E^2|B|$

LOFAR LOw Frequency ARray

- **Giant digital & multi-purpose radio telescope** distributed across Europe
- **Radio interferometer** composed of **~48 phased arrays** (stations)
- Working bands: **LBA** 30-80 MHz & **HBA** 120-240 MHz
- **Improved angular** (arcsec)**, temporal** (μs), **spectral** (kHz) resolutions
- **High sensitivity** (~mJy) 1 Jy = 10^{-26} W.m^{-2}.Hz^{-1}

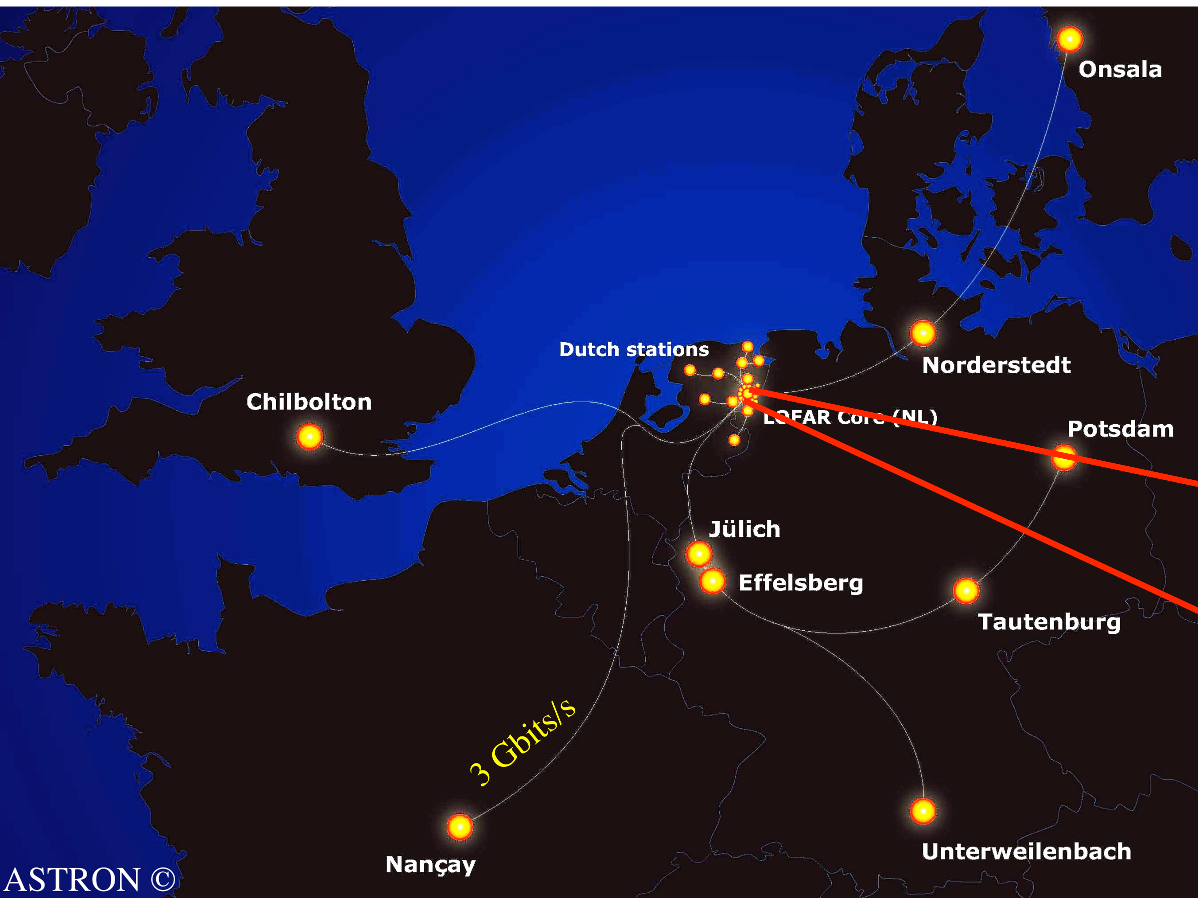

Observing strategy with LOFAR

- 10 consecutives hours (~1 rotation) $D_E = 3.29°$
- HBA F = 127-172 MHz
- 29 NL stations
- 2 // beams : Jupiter & phase calibrator 4° away
- $\delta t = 0.3$ ms , $\delta f = 3$ kHz
- Full Stokes measurement

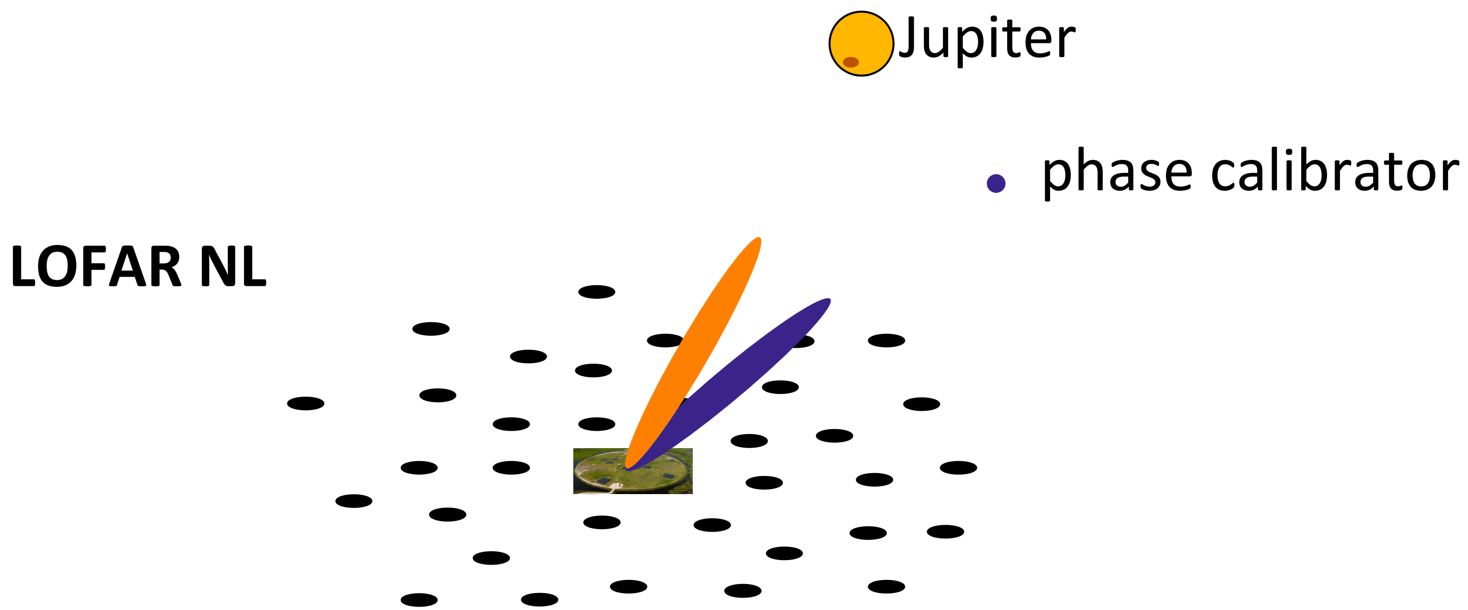

Data processing

LOFAR = wide Field of View instrument

Planetary imaging = « classical » radio imaging + specificities

- Proper motion of the planet on the sky

- Intrinsic motion of the radiations belts around the planet

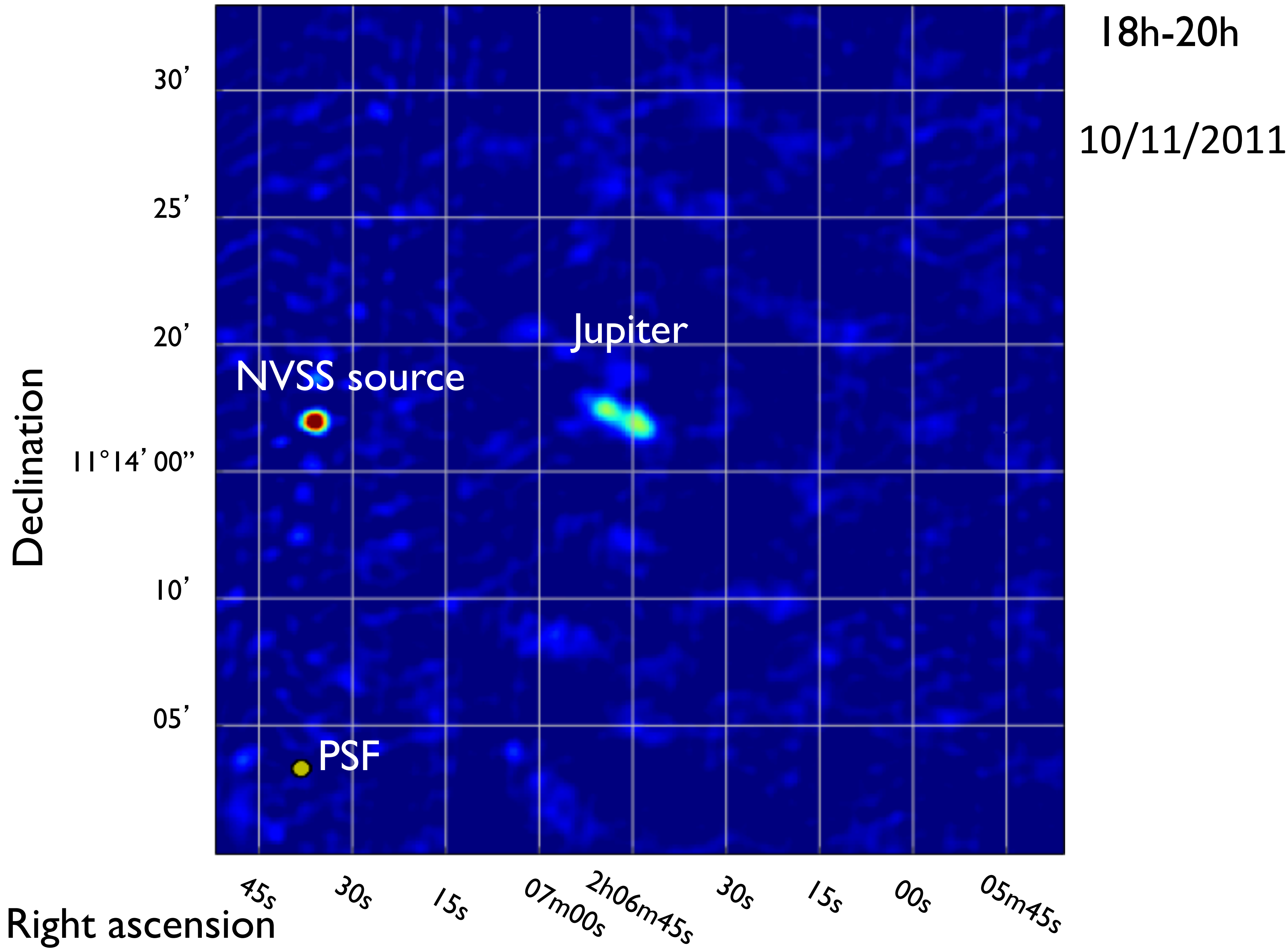
18h-20h
10/11/2011
Jupiter
NVSS source
PSF
Declination
30'
25'
20'
11°14' 00"
10'
05'
45s
30s
15s
07m00s
2h06m45s
30s
15s
00s
05m45s
Right ascension

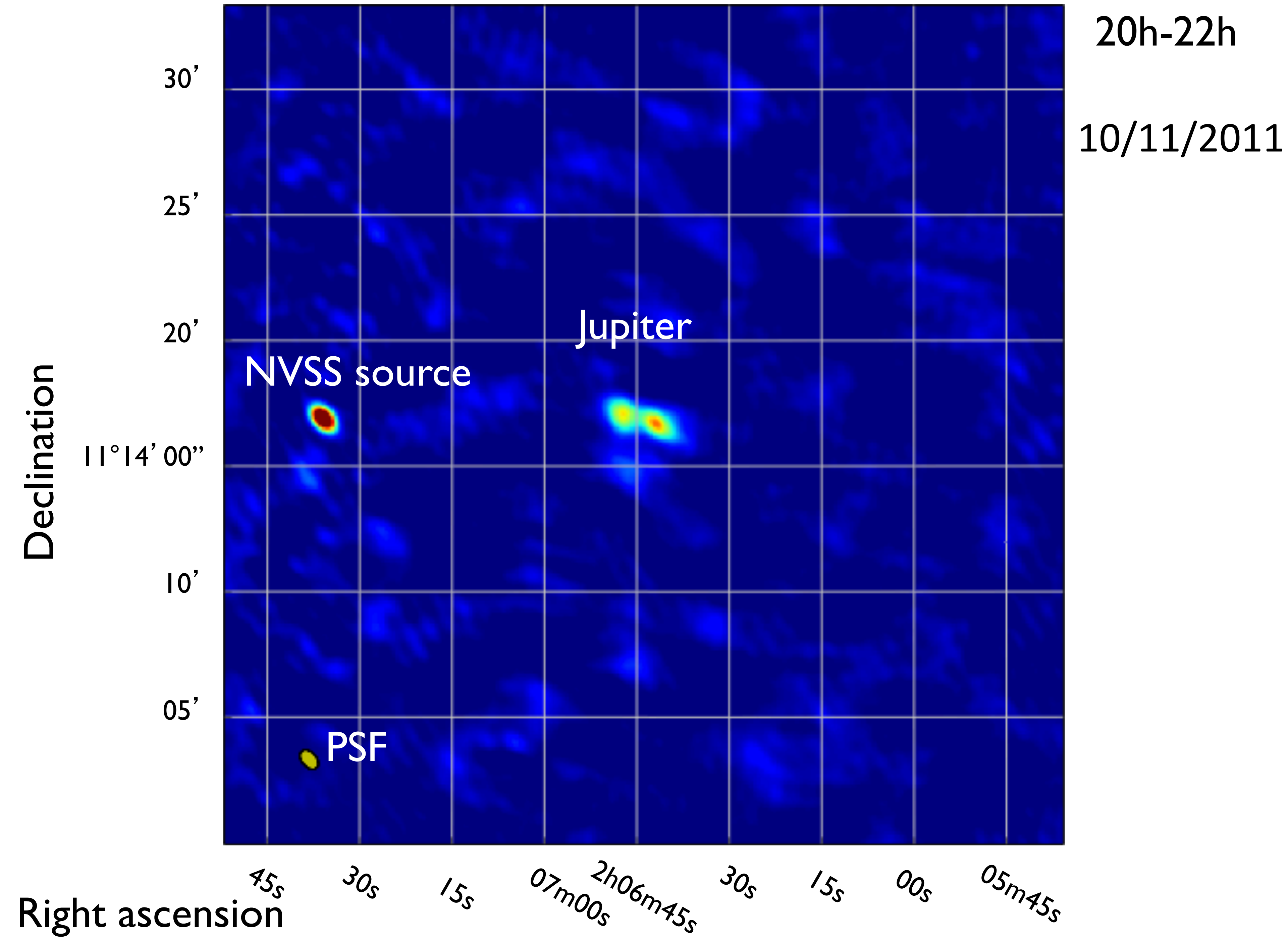

20h-22h
10/11/2011
Jupiter
NVSS source
PSF
Declination
30'
25'
20'
11°14' 00"
10'
05'
Right ascension
45s
30s
15s
07m00s
2h06m45s
30s
15s
00s
05m45s

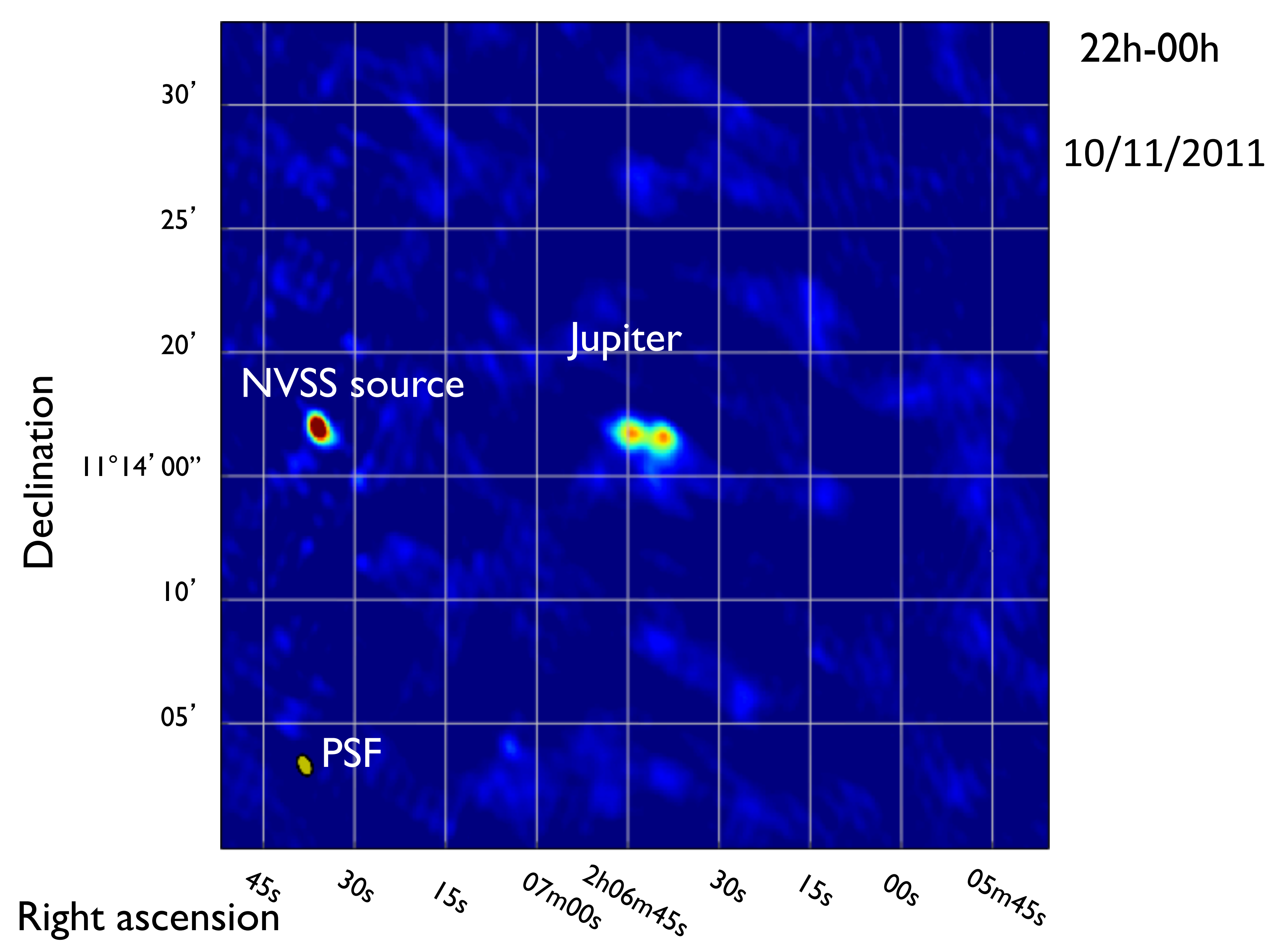
22h-00h
10/11/2011
Jupiter
NVSS source
PSF
Declination
30'
25'
20'
11°14' 00"
10'
05'
Right ascension
45s
30s
15s
07m00s
2h06m45s
30s
15s
00s
05m45s

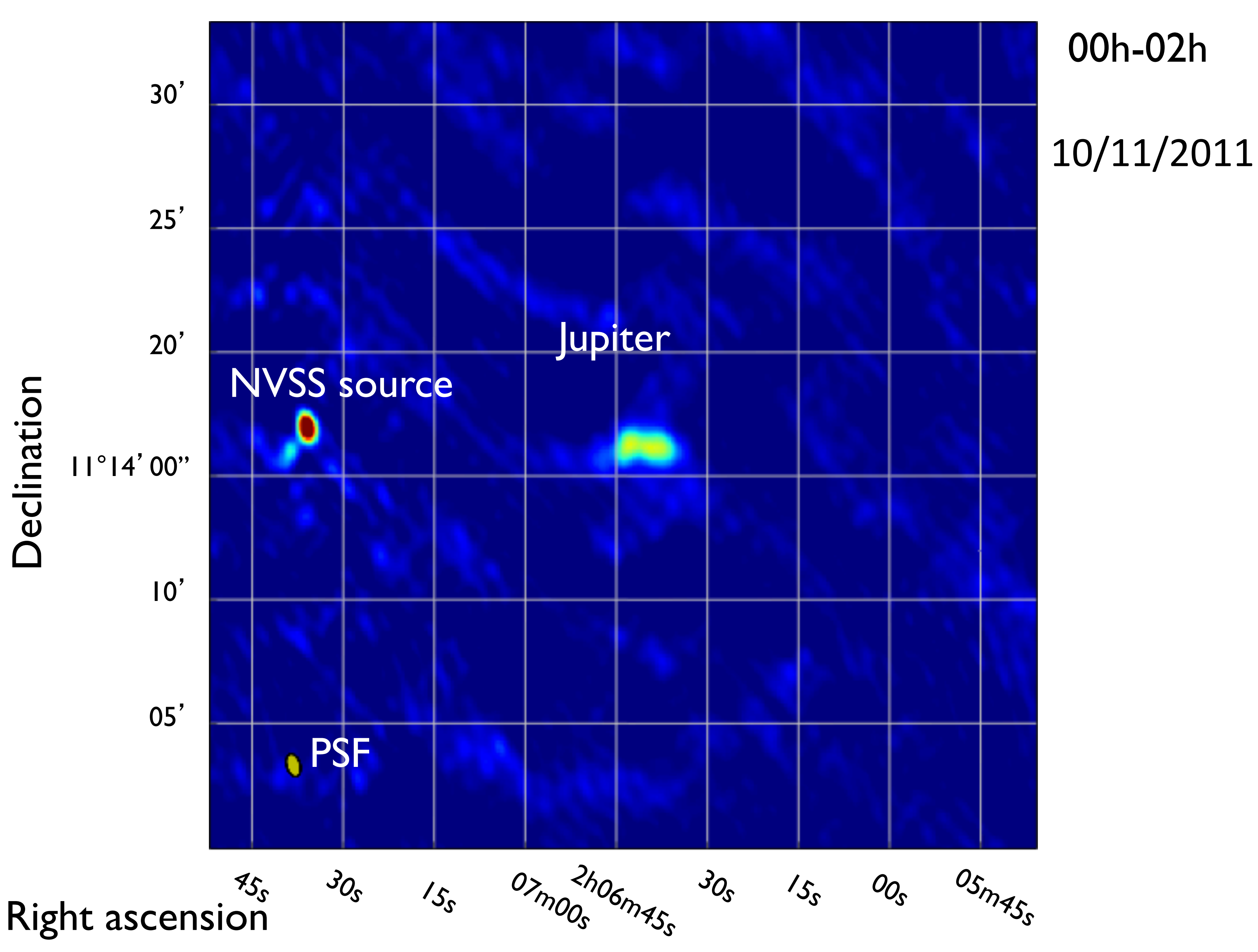
00h-02h
10/11/2011
Jupiter
NVSS source
PSF
Declination
30'
25'
20'
11°14' 00"
10'
05'
Right ascension
45s
30s
15s
07m00s
2h06m45s
30s
15s
00s
05m45s

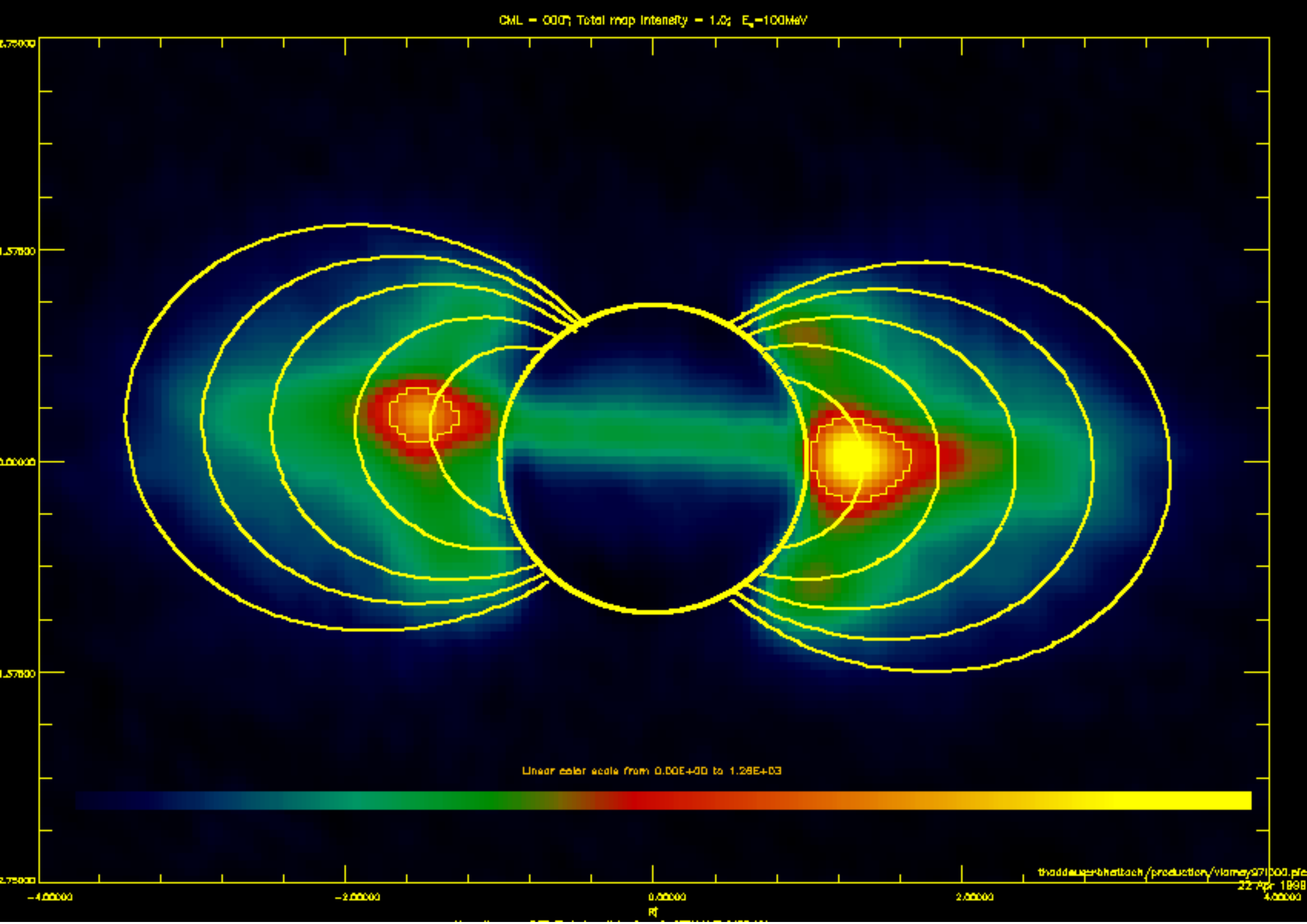

[Levin et al., 2001]

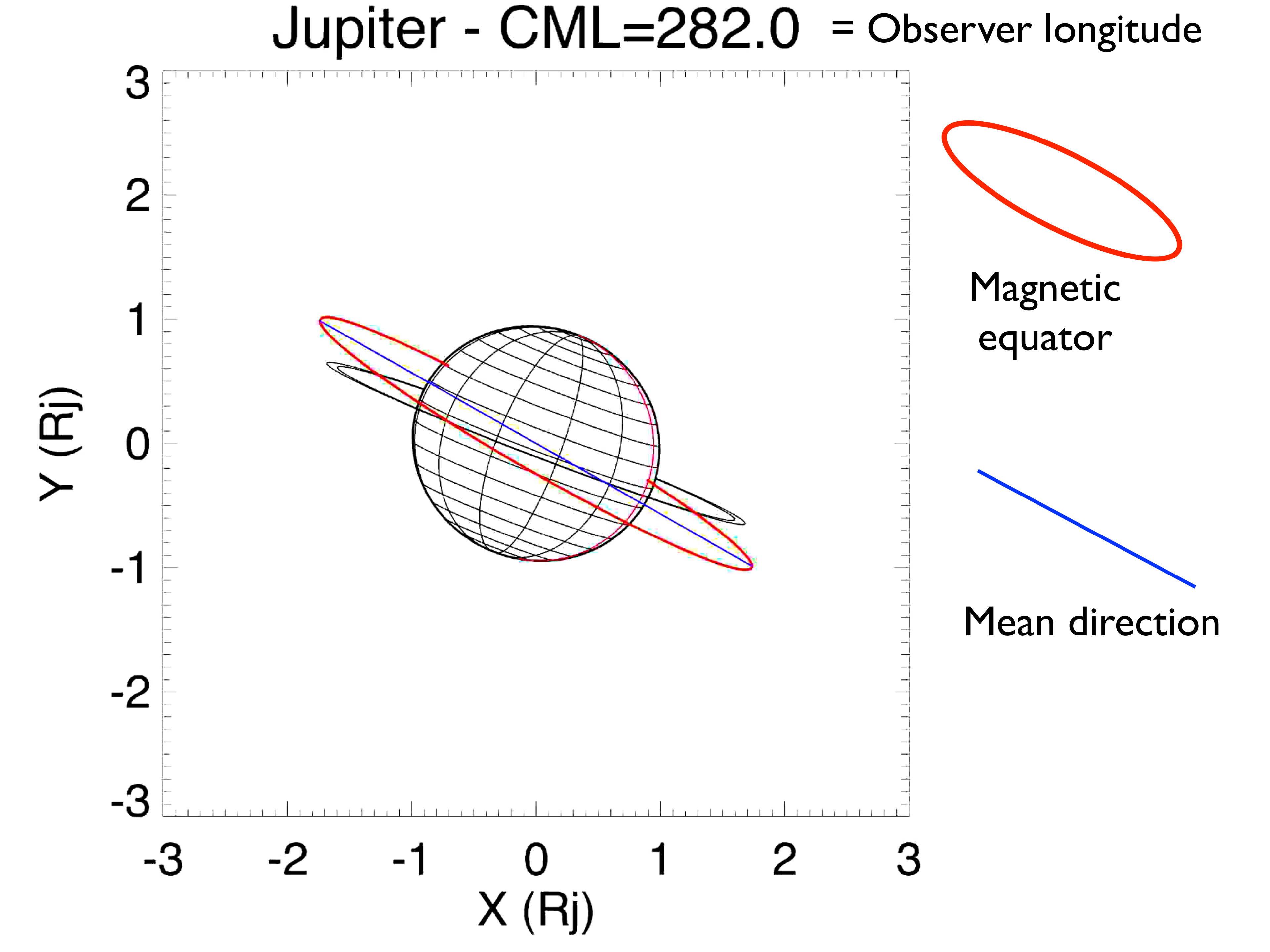

Jupiter - CML=282.0
= Observer longitude
Y (Rj)
X (Rj)
3
2
1
0
-1
-2
-3
Magnetic equator
Mean direction

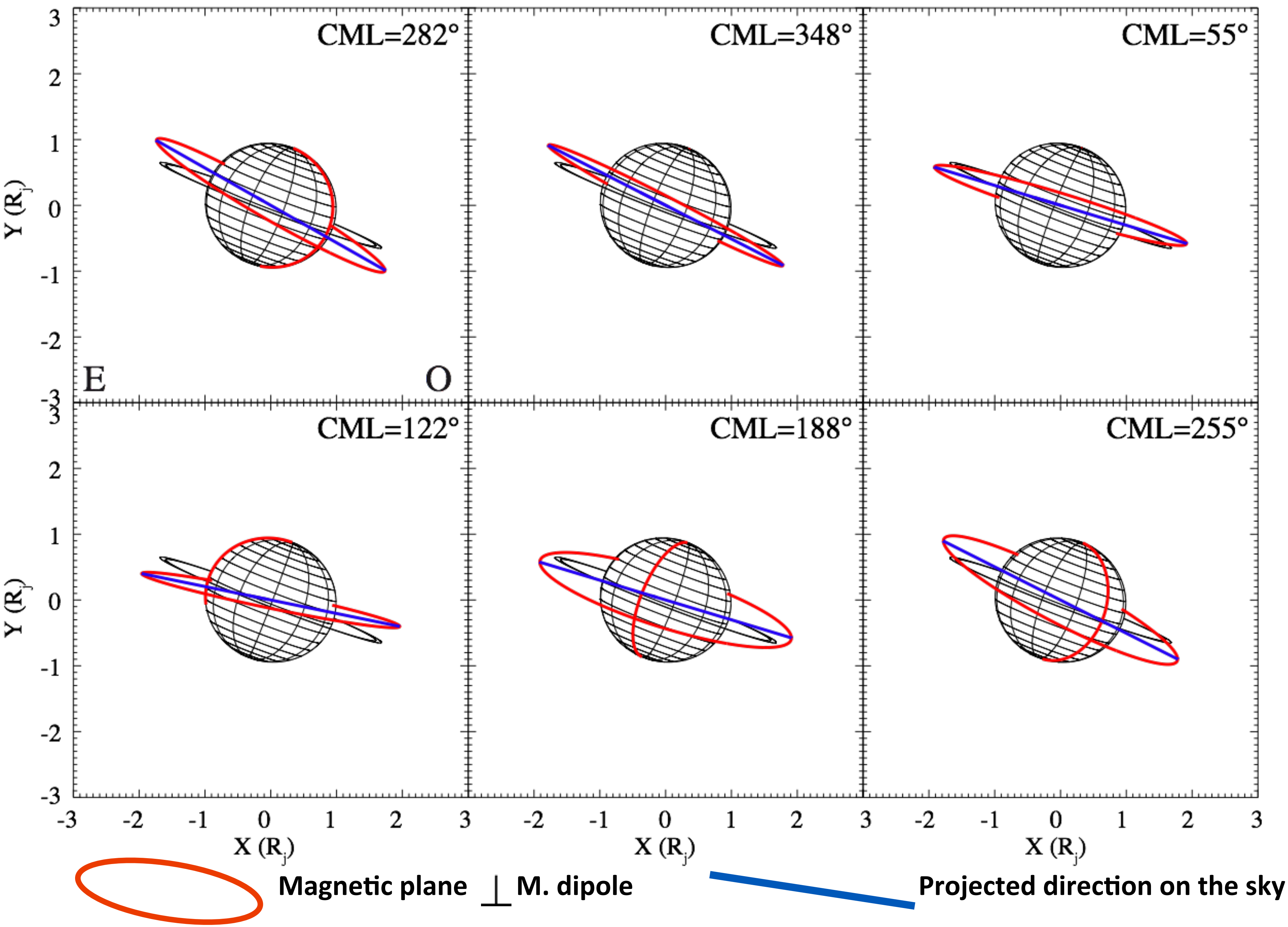
CML=282°
CML=348°
CML=55°
CML=122°
CML=188°
CML=255°
E
O
Y (R$_j$)
X (R$_j$)
Magnetic plane ⊥ M. dipole
Projected direction on the sky

Data processing

LOFAR = wide Field of View instrument

Planetary imaging = « classical » radio imaging + specificities

- Proper motion of the planet on the sky

→ Phase center correction in the Fourier domain

- Intrinsic motion of the radiations belts around the planet

→ Rotation correction in the Fourier domain

only on Jupiter

→ Prior: wide-field imaging and source substraction (peeling)

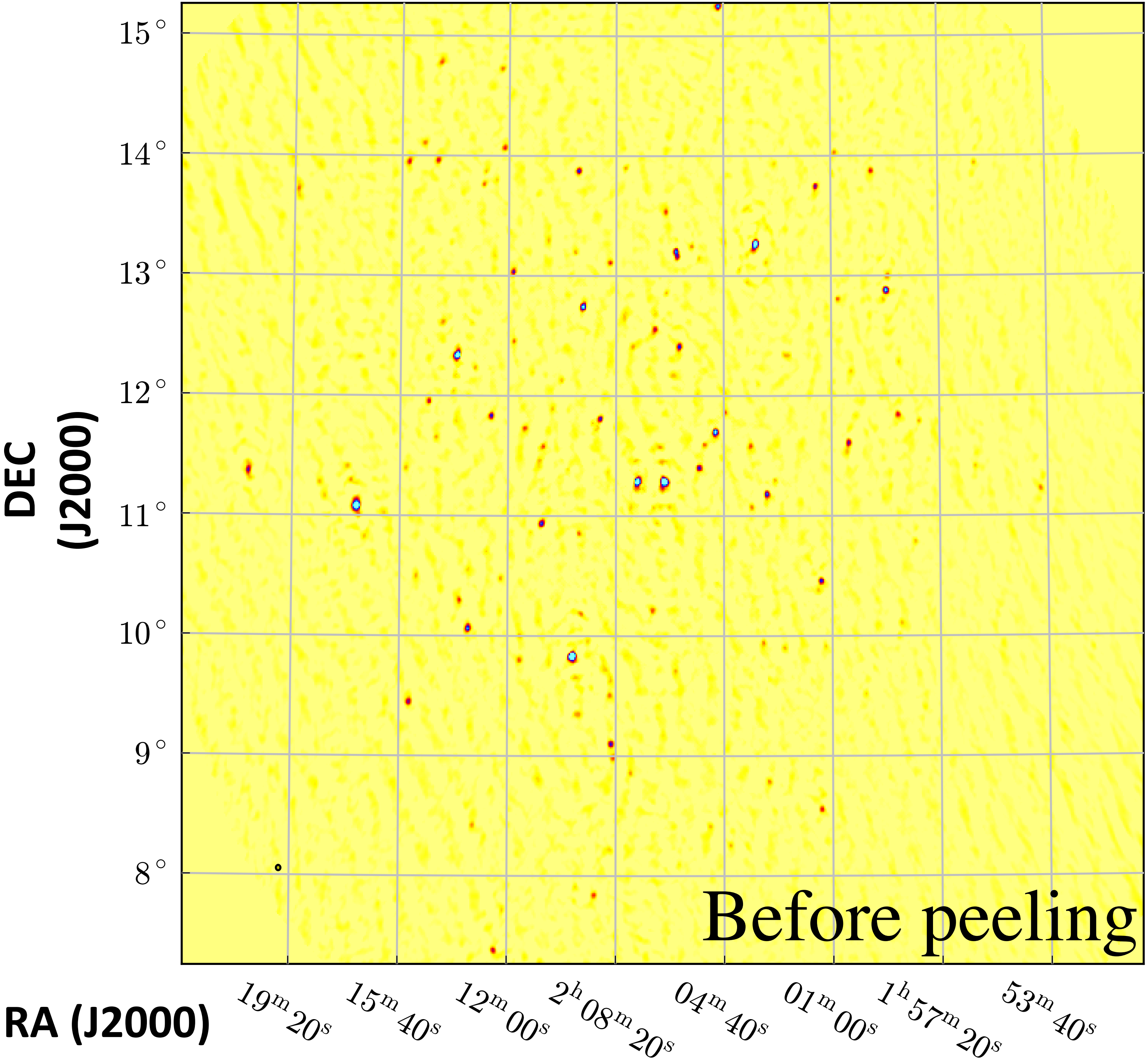
DEC (J2000)
15°
14°
13°
12°
11°
10°
9°
8°
RA (J2000)
19m20s
15m40s
12m00s
2h08m20s
04m40s
01m00s
1h57m20s
53m40s
Before peeling

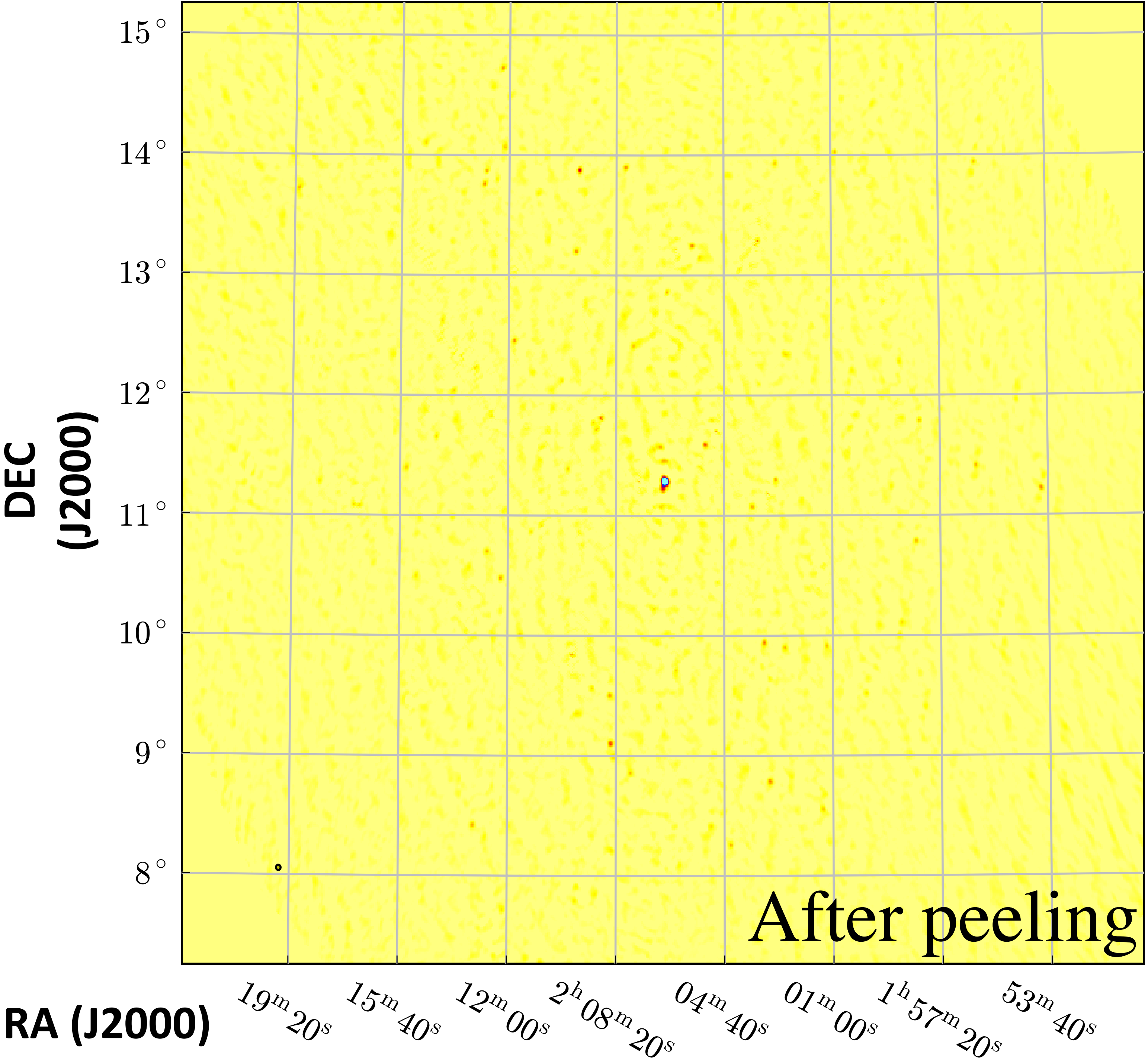
DEC (J2000)
RA (J2000)
15°
14°
13°
12°
11°
10°
9°
8°
19m20s
15m40s
12m00s
2h08m20s
04m40s
01m00s
1h57m20s
53m40s
After peeling

Data processing

LOFAR = wide Field of View instrument

Planetary imaging = « classical » radio imaging + specificities

- Proper motion of the planet on the sky

→ Phase center correction in the visibility plane

- Intrinsic motion of the radiations belts around the planet

→ Rotation correction in the visibility plane

☝ only on Jupiter

→ Prior: wide-field imaging and source substraction (peeling)

- after corrections → image data cubes

Resolved intensity maps

- Integration over 127-172 MHz, $\Delta t = 2h$,
- After the geometric corrections on the visibility plane

  → corrections are OK

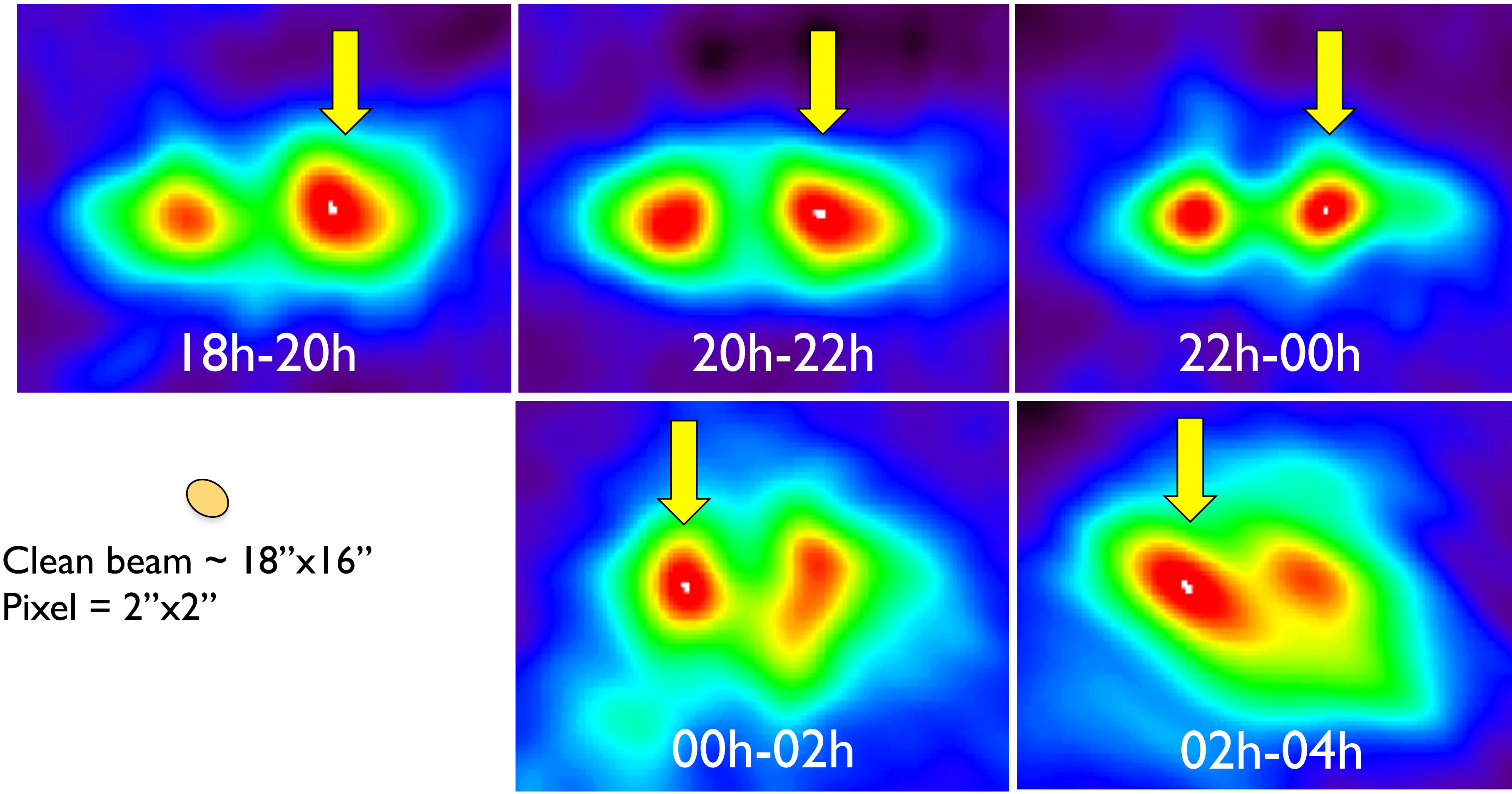

Clean beam ~ 18”x16”
Pixel = 2”x2”

Resolved intensity maps

- Integration over 127-172 MHz, Δt = 7h

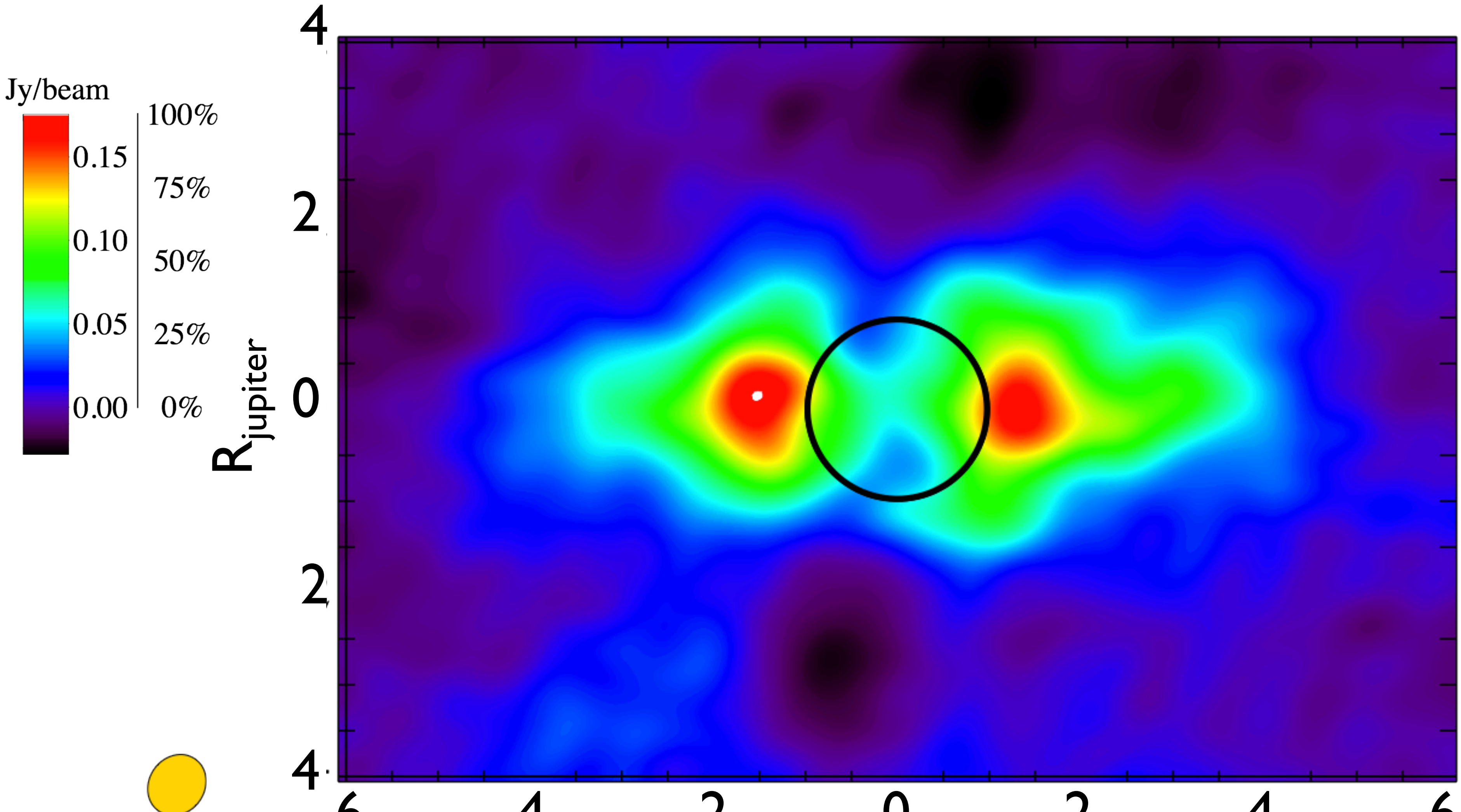

Clean beam = 18”x16”
Pixel = 1”x1”

Resolved intensity maps

- Integration over 127-172 MHz, Δt = 7h

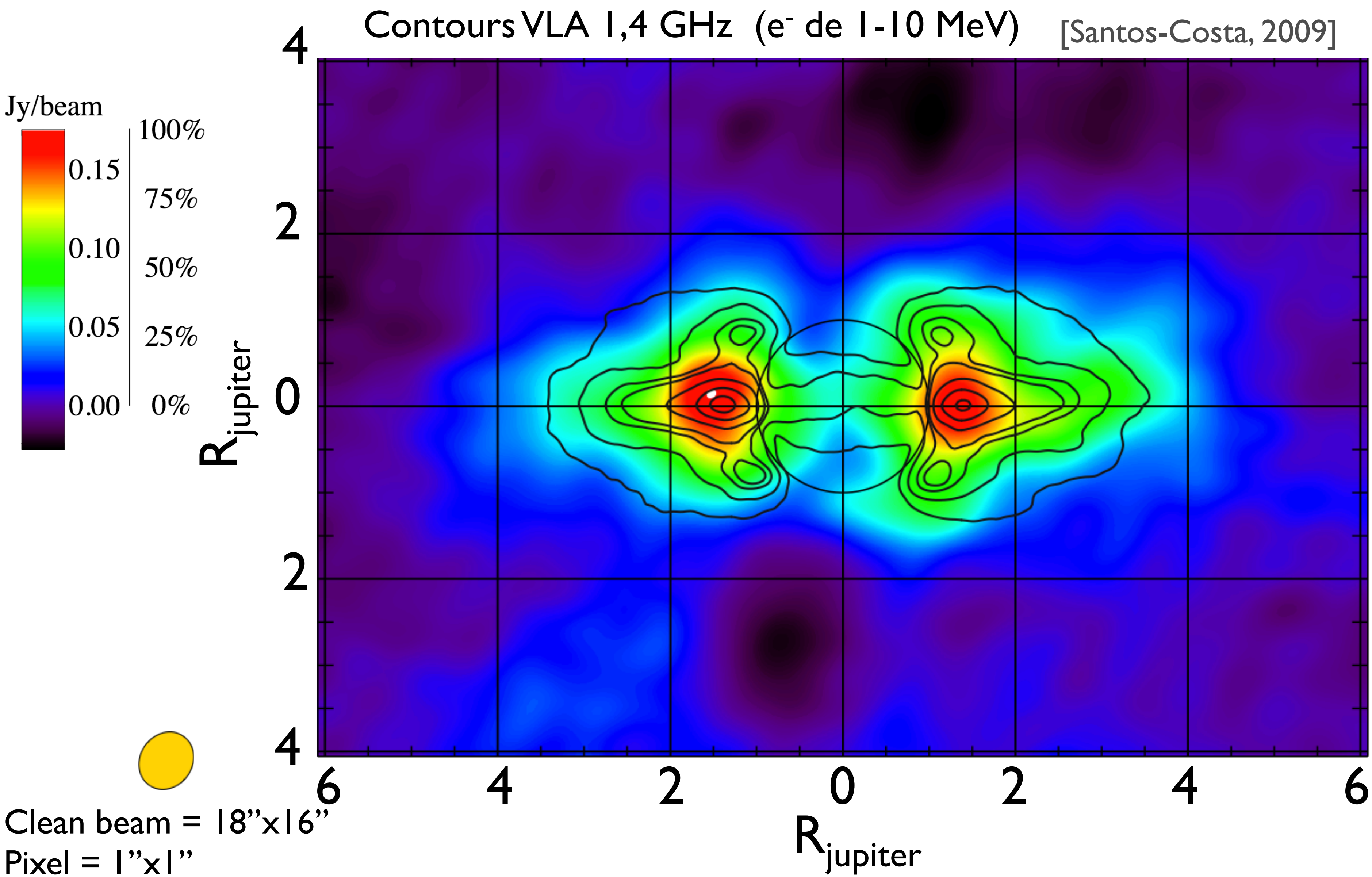

Clean beam = 18”x16”
Pixel = 1”x1”

Resolved intensity maps

- Integration over 127-172 MHz, Δt = 7h

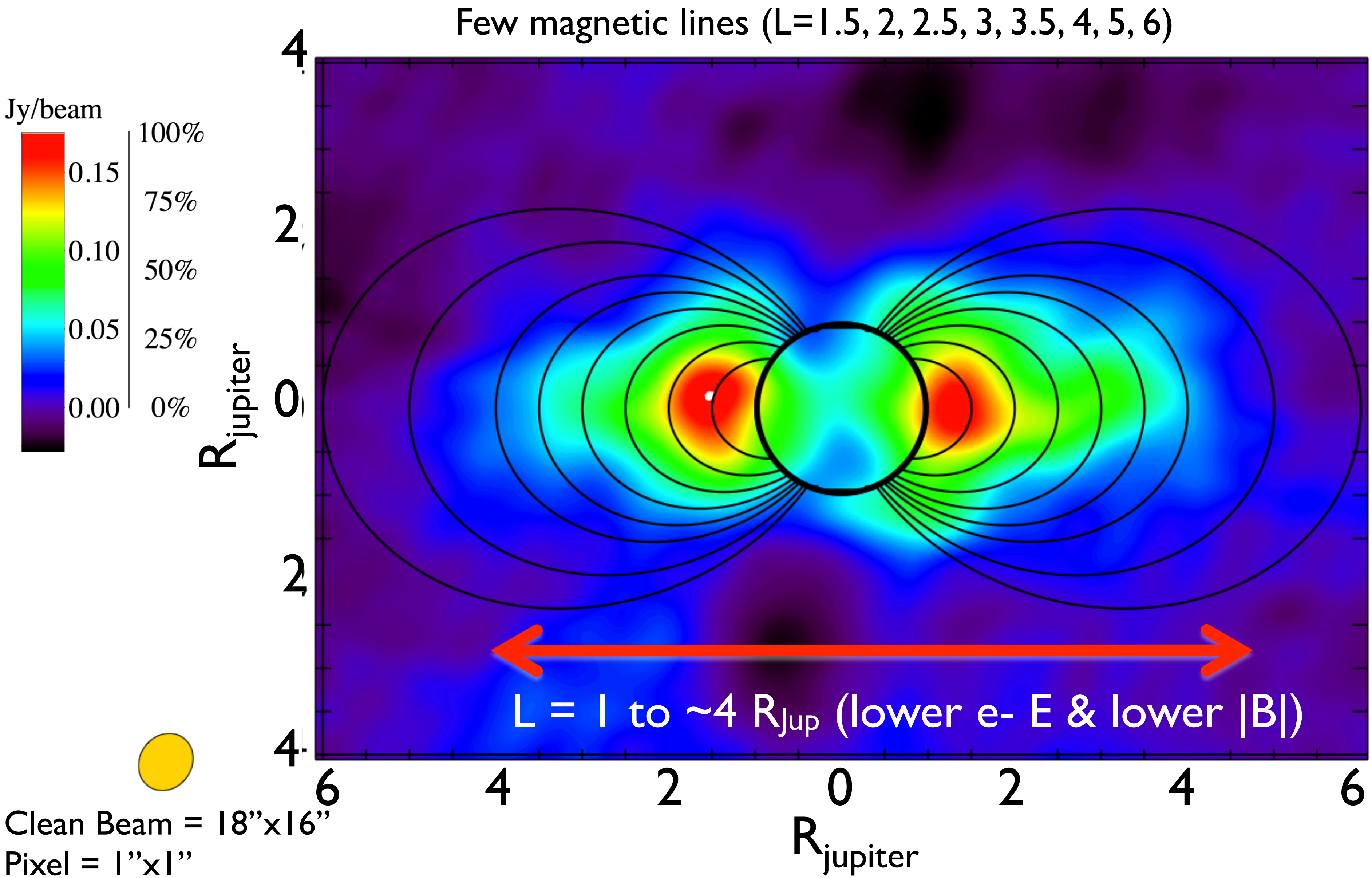

Clean Beam = 18”x16”

Pixel = 1”x1”

LF morphological properties of the belts

East peak | West peak

Peak position with frequency

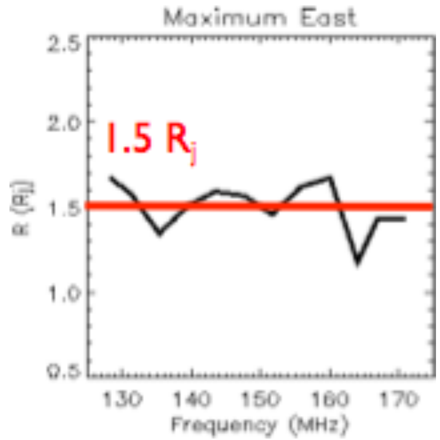

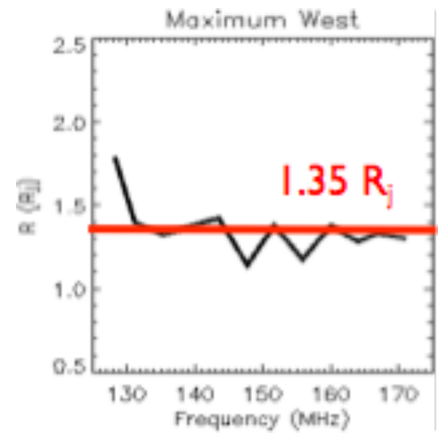

→East-West asym.

→sim to VLA at 5 GHz

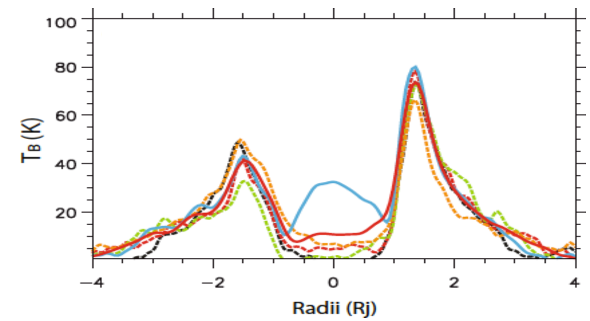

[Santos-Costa et al., 2009]

Peak position with time

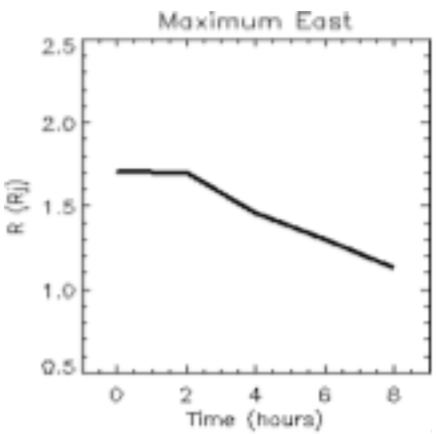

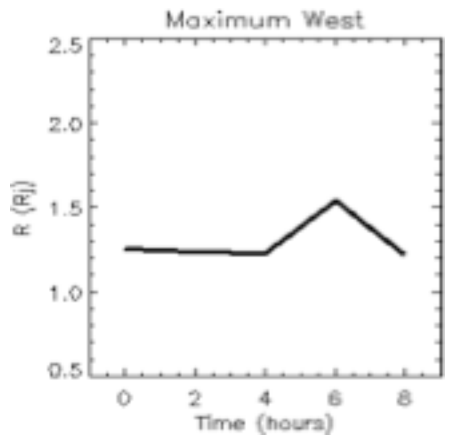

→ geometrical effect

radial excursions measured at HF ~0.25 R_j from 1.45 to 1.7 R_j

[Dulk et al., 1997]

«Hot spot» tracking

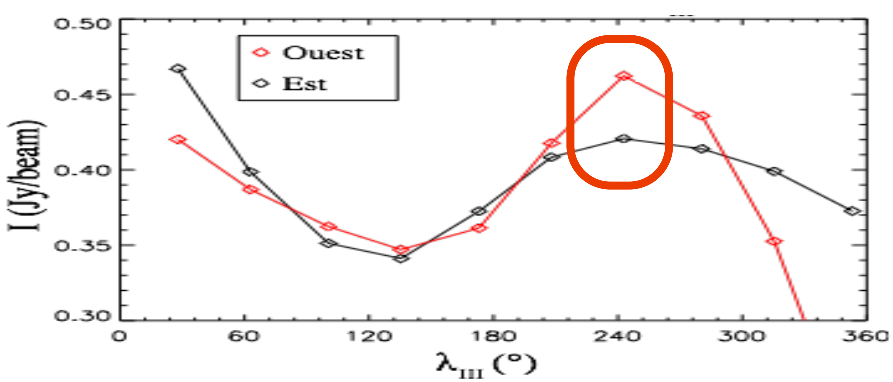

→max ~230°±25°

→idem @ HF

[Conway & Stannard, 1972]
[de Pater, 1983]
[Leblanc, 1997]

[Girard et al., in prep.]

Integrated flux density

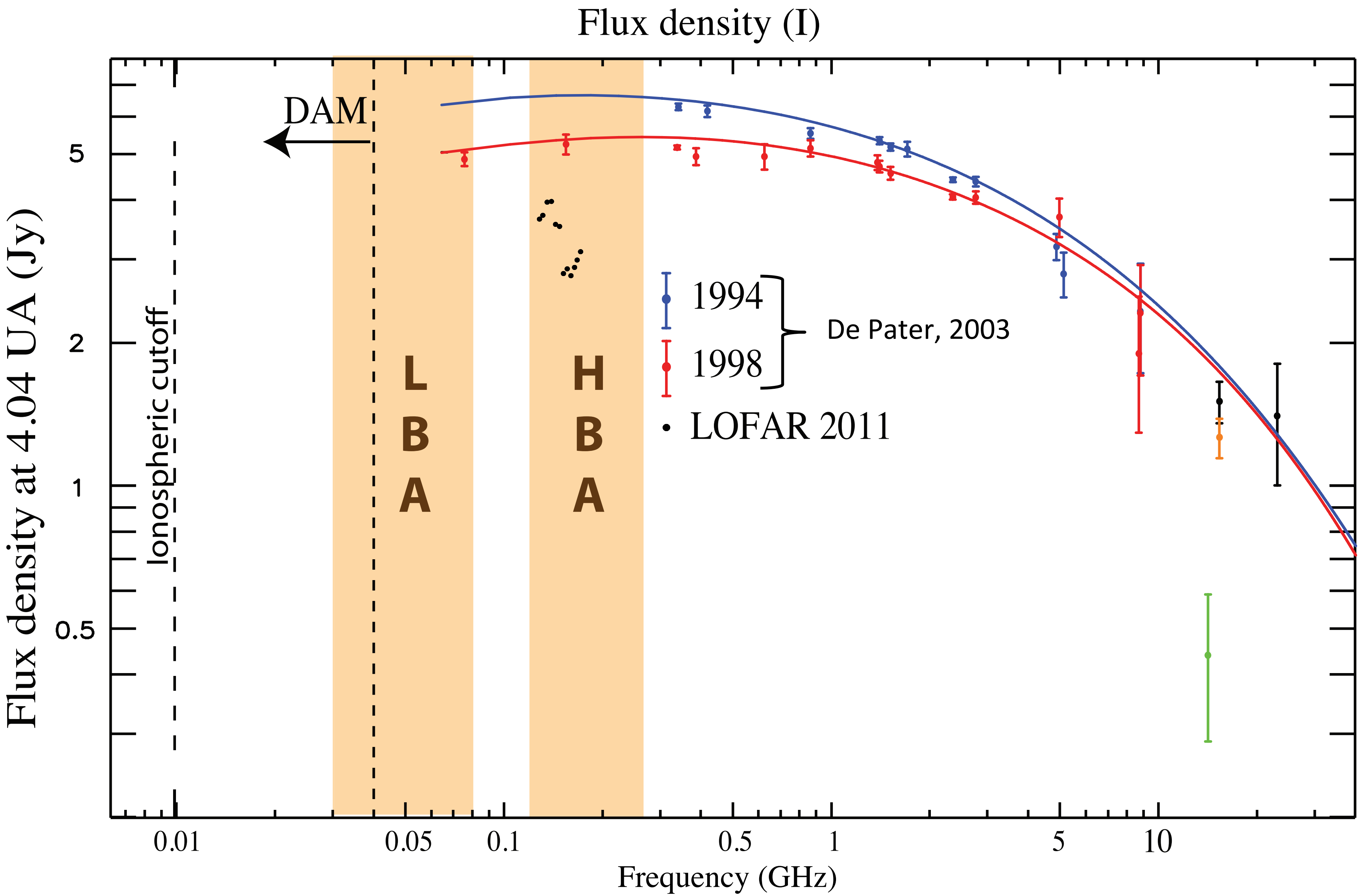

[adapted from de Pater et al., 2003]

Integrated flux density

- **Nearby sources around Jupiter in data before source substraction**

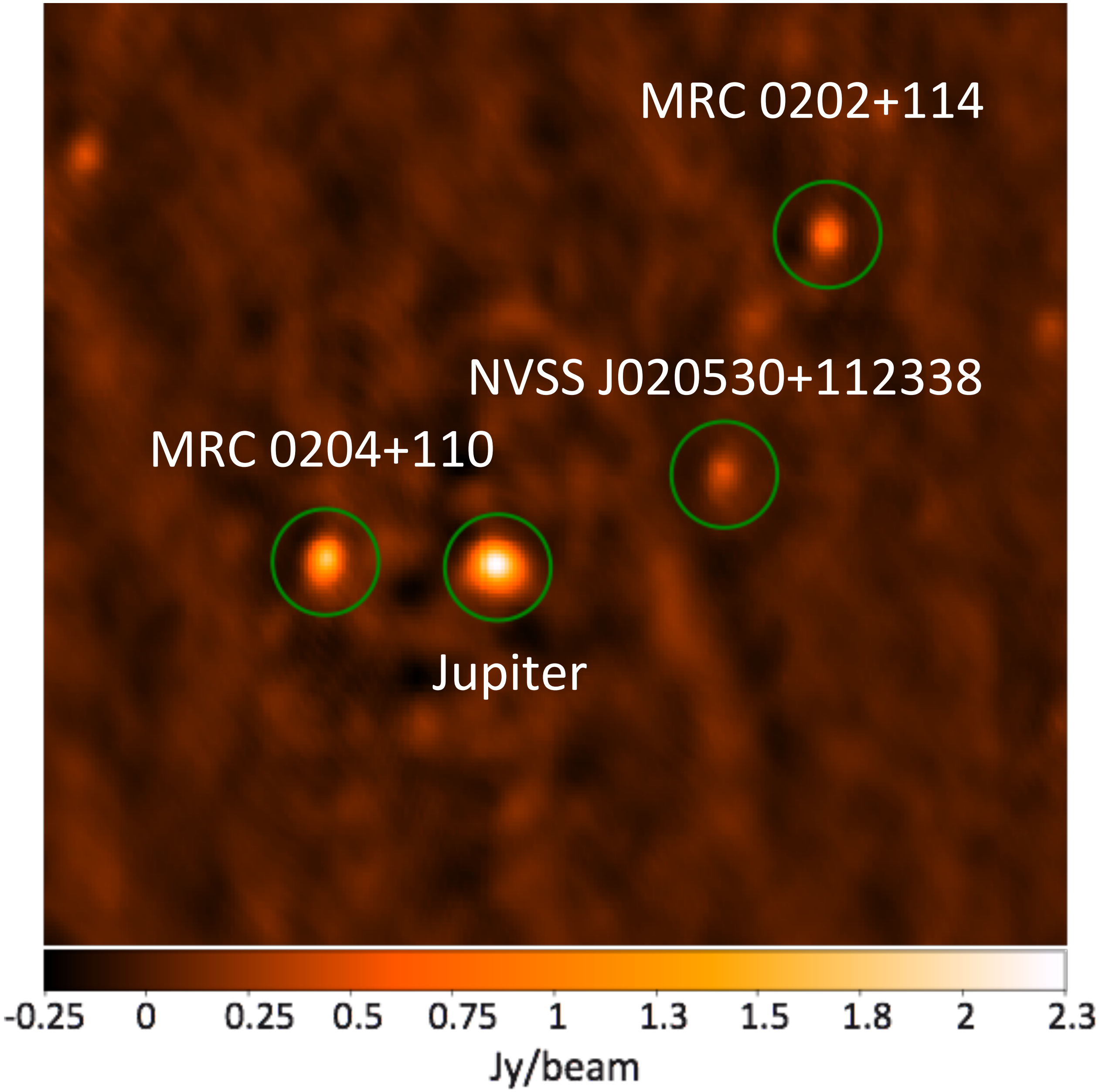

Integrated flux density

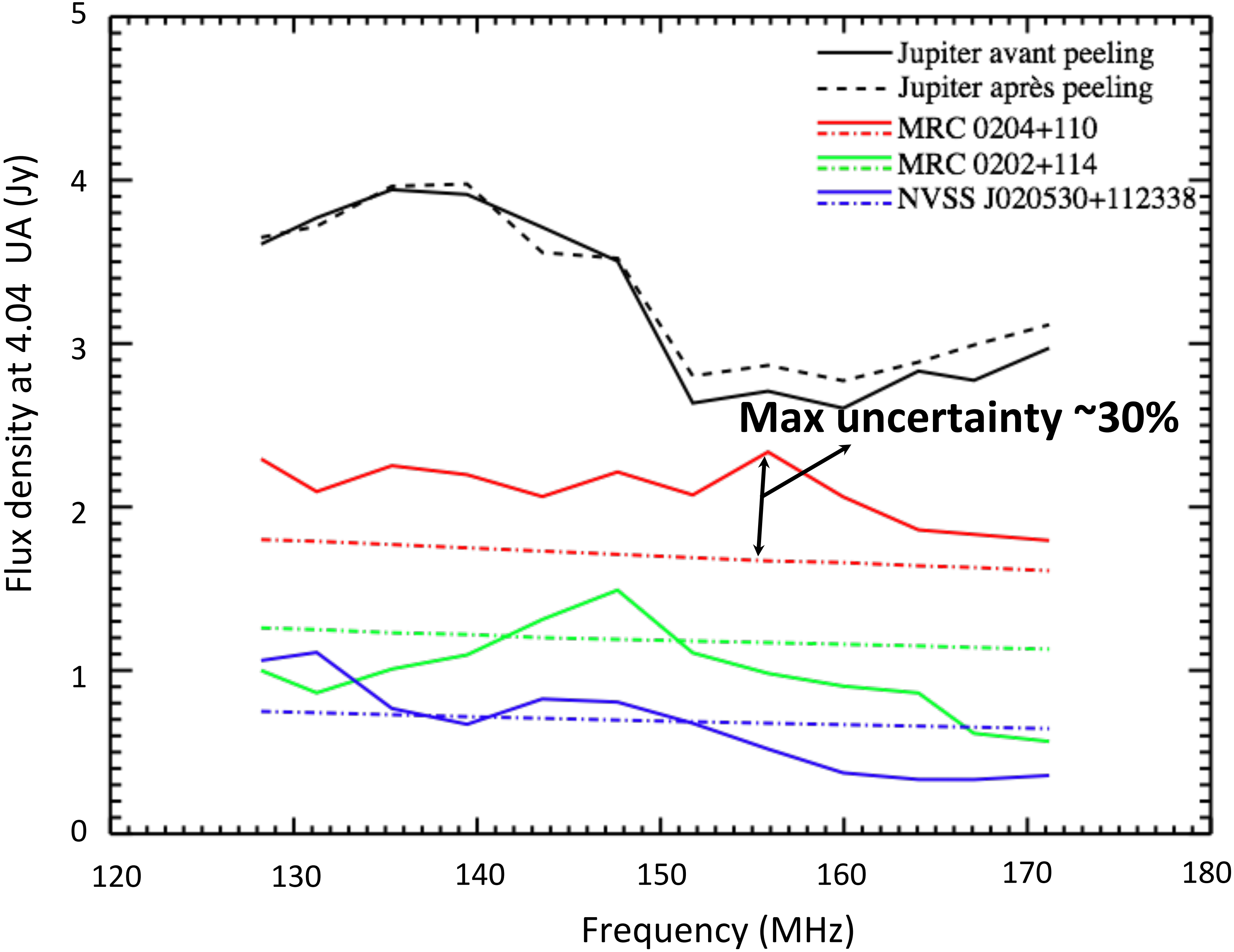

Integrated flux density

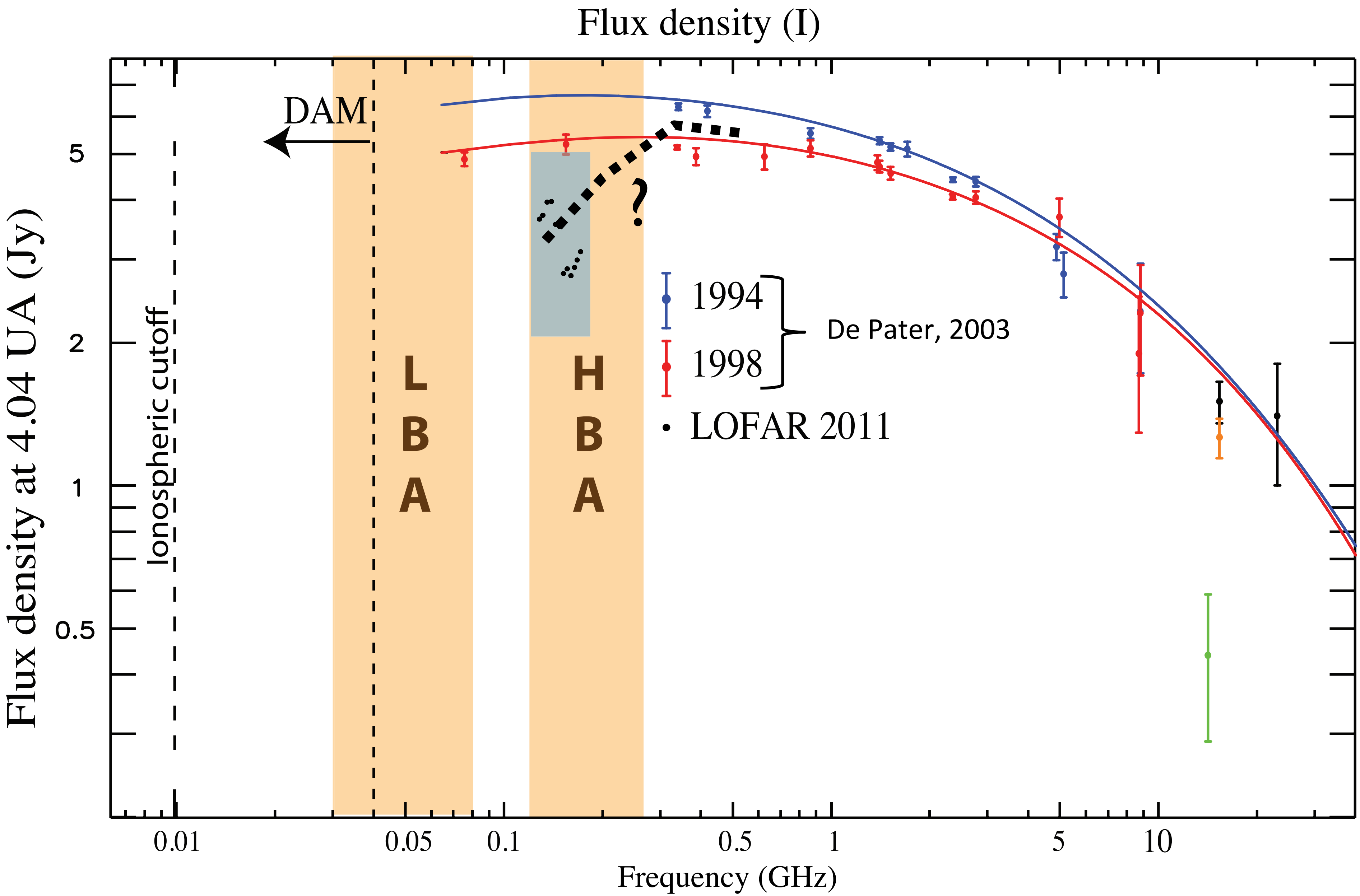

[adapted from de Pater et al., 2003]

Integrated flux density

- Feb 19-20th, 2013
- Broad frequency coverage: 6 m ↔ 6 cm

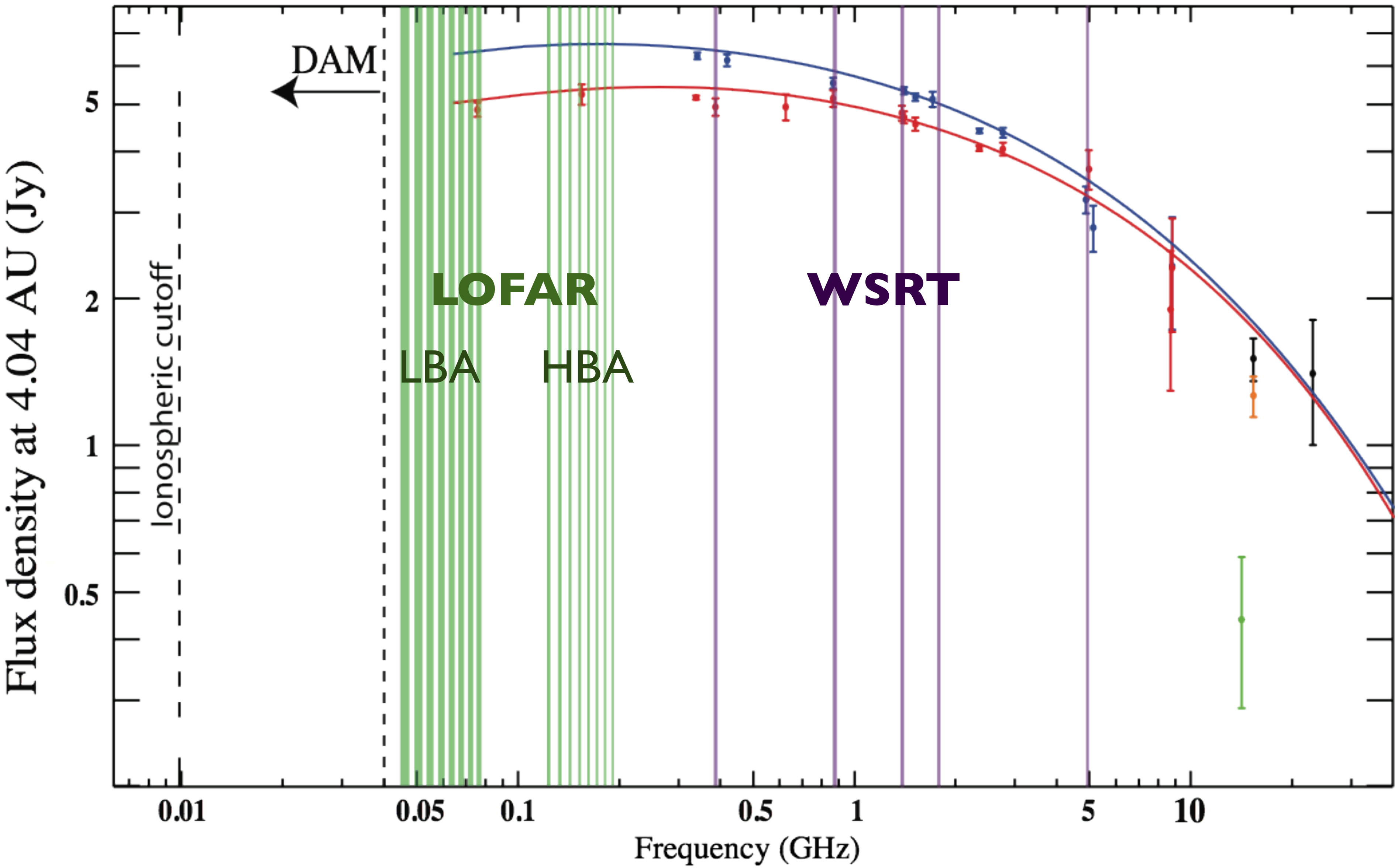

On going work...

LBA

F=55 MHz - 10 SB - 37 stat - 2h

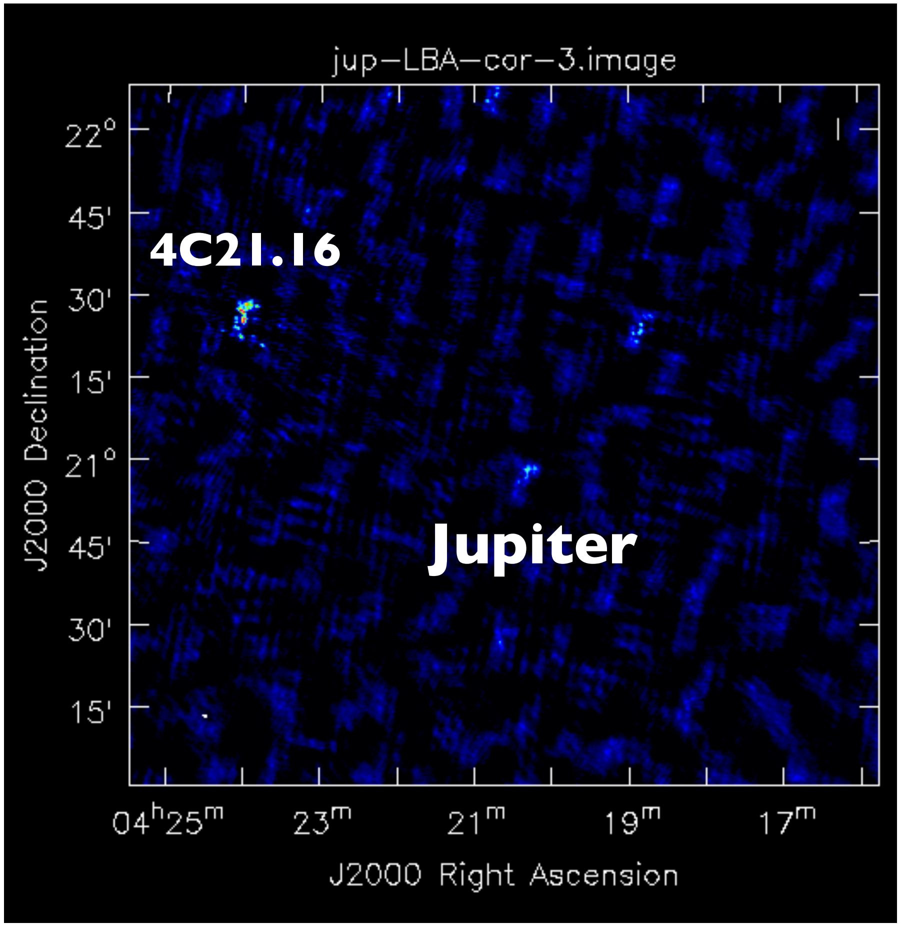

HBA

F=149MHz - 15 SB - 57 stat (HBA DUAL) - 2h

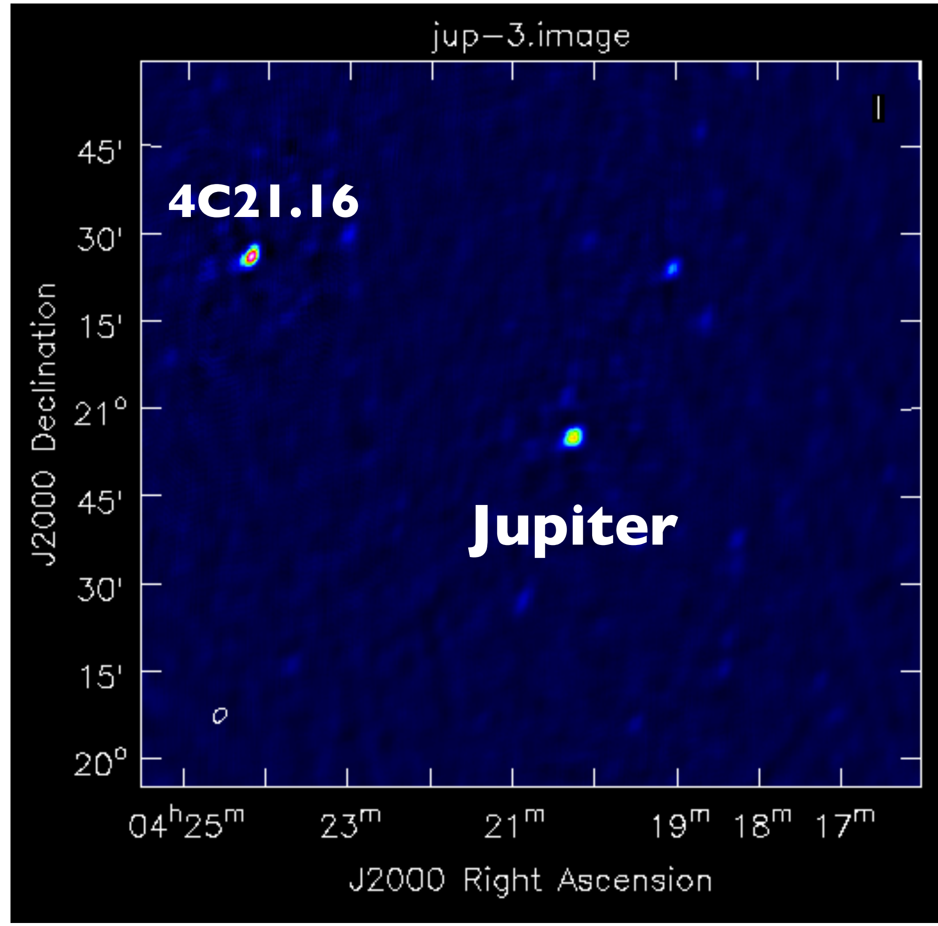

- full study on-going...

  spectrum, resolved emission, comp. with WSRT, temporal variability...

Integrated flux density

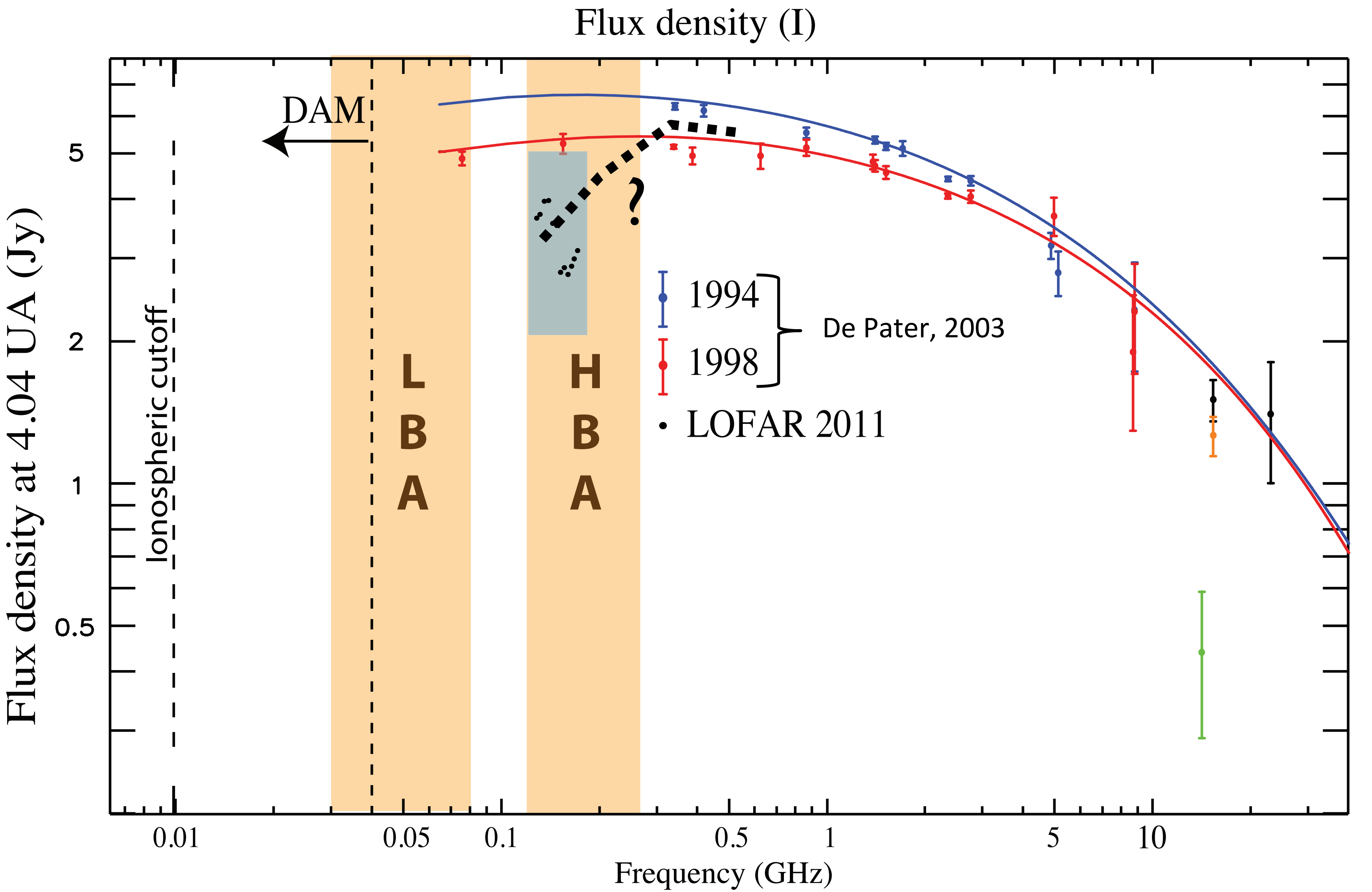

[adapted from de Pater et al., 2003]

Integrated flux density

Preliminary

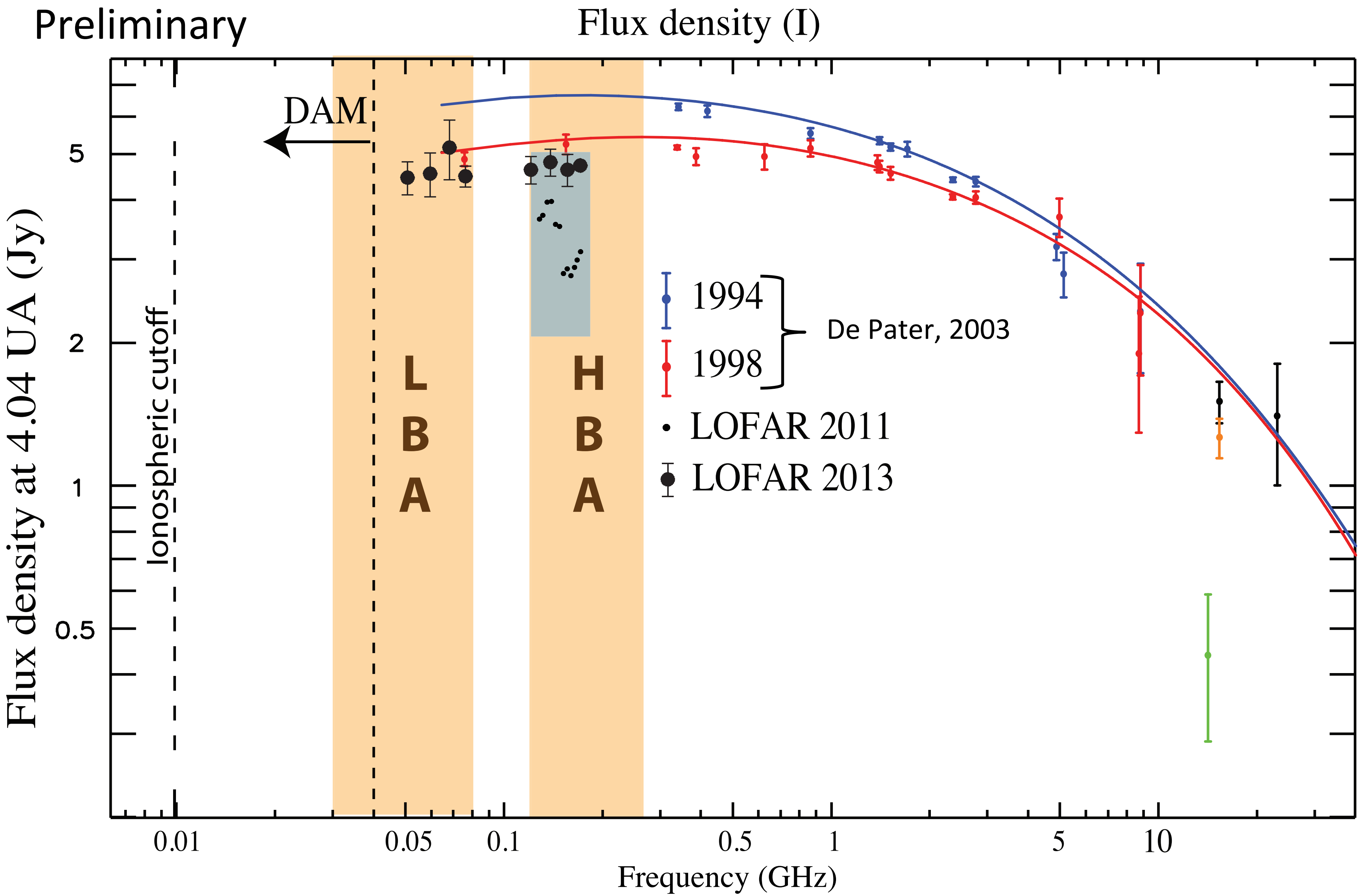

[adapted from de Pater et al., 2003]

Integrated flux density

Preliminary

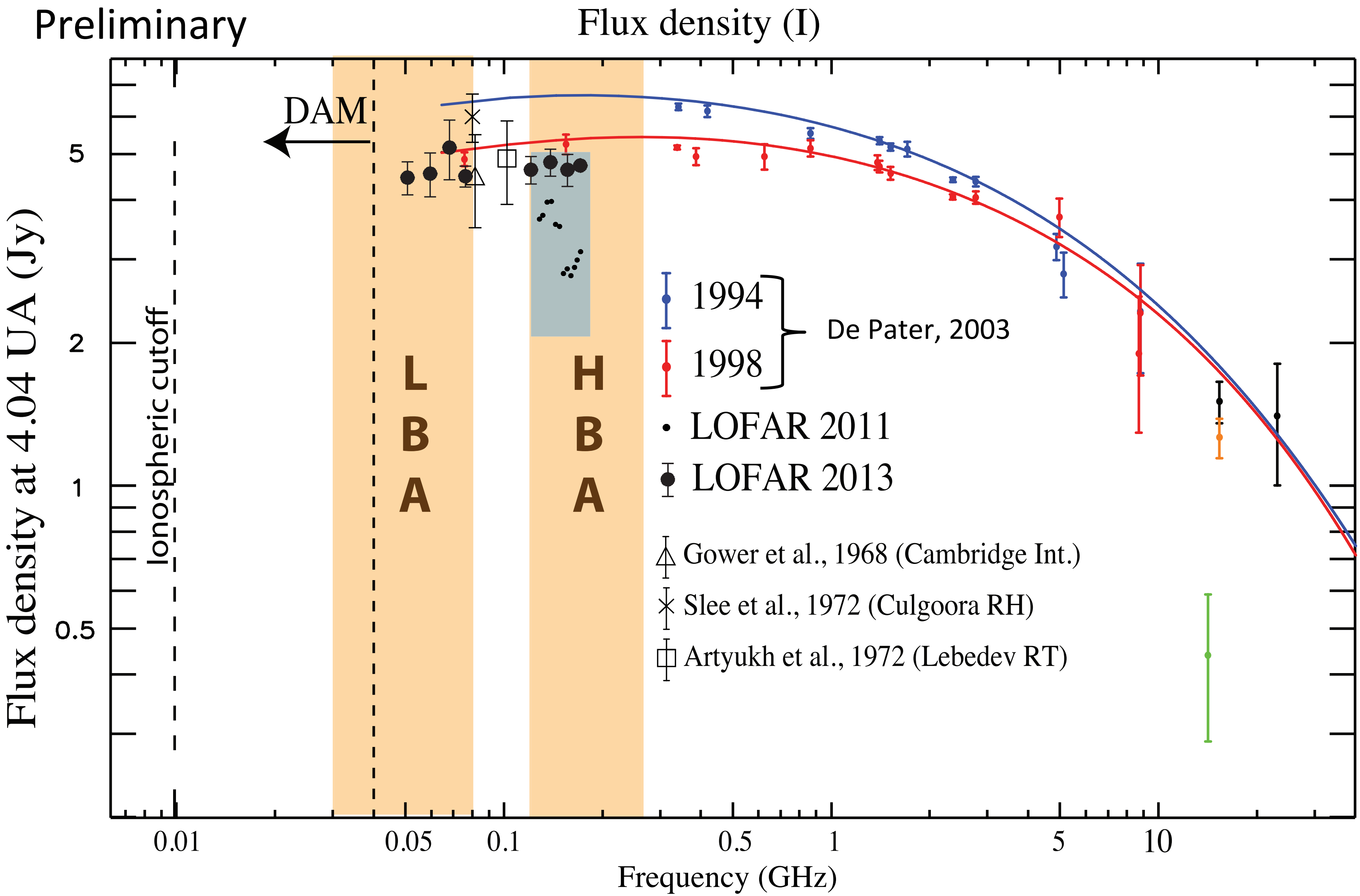

[adapted from de Pater et al., 2003]

Conclusions (so far)

- LOFAR, flexible planetary imager
- First resolved images < 200 MHz
- Larger extent of the belts at LF
- Basic morphological properties
- Potential (temporal) variation of the spectrum

Prospects

- Full (instantaneous) spectrum
- Short and long-term variability
- Polarization
- Comparison with Salammbô (ONERA)
- 3D Reconstruction (by tomography)

→ Distribution, transport/source/loss processes of (low energy) e⁻

→ Topology of the inner magnetic field

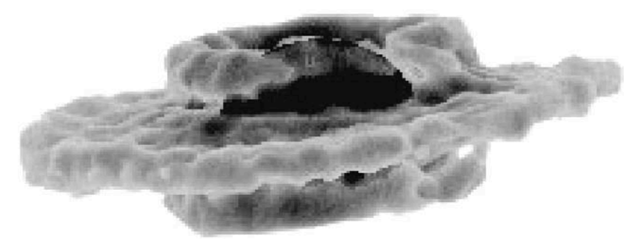

[de Pater & Sault, 1998]

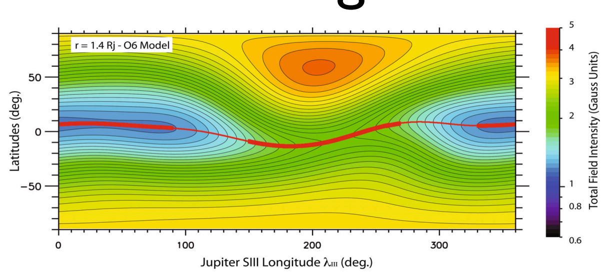

[Connerney et al., 1993 ; Santos-Costa, 2009]

France-Berkeley Fund proposal submitted in January for this study

What about Saturn with LOFAR?

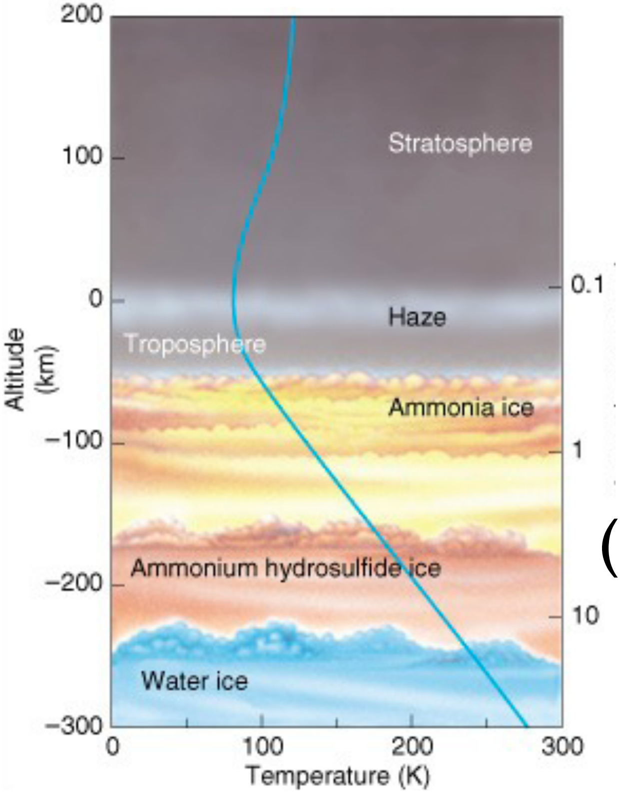

Saturn thermal emission

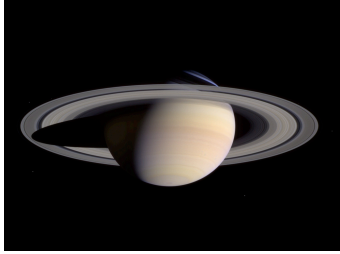

- Probe deeply into Saturn atmosphere
- Measuring the abundance of water
- Expected flux density: 2-10 mJy

Contribution to the thermal emission

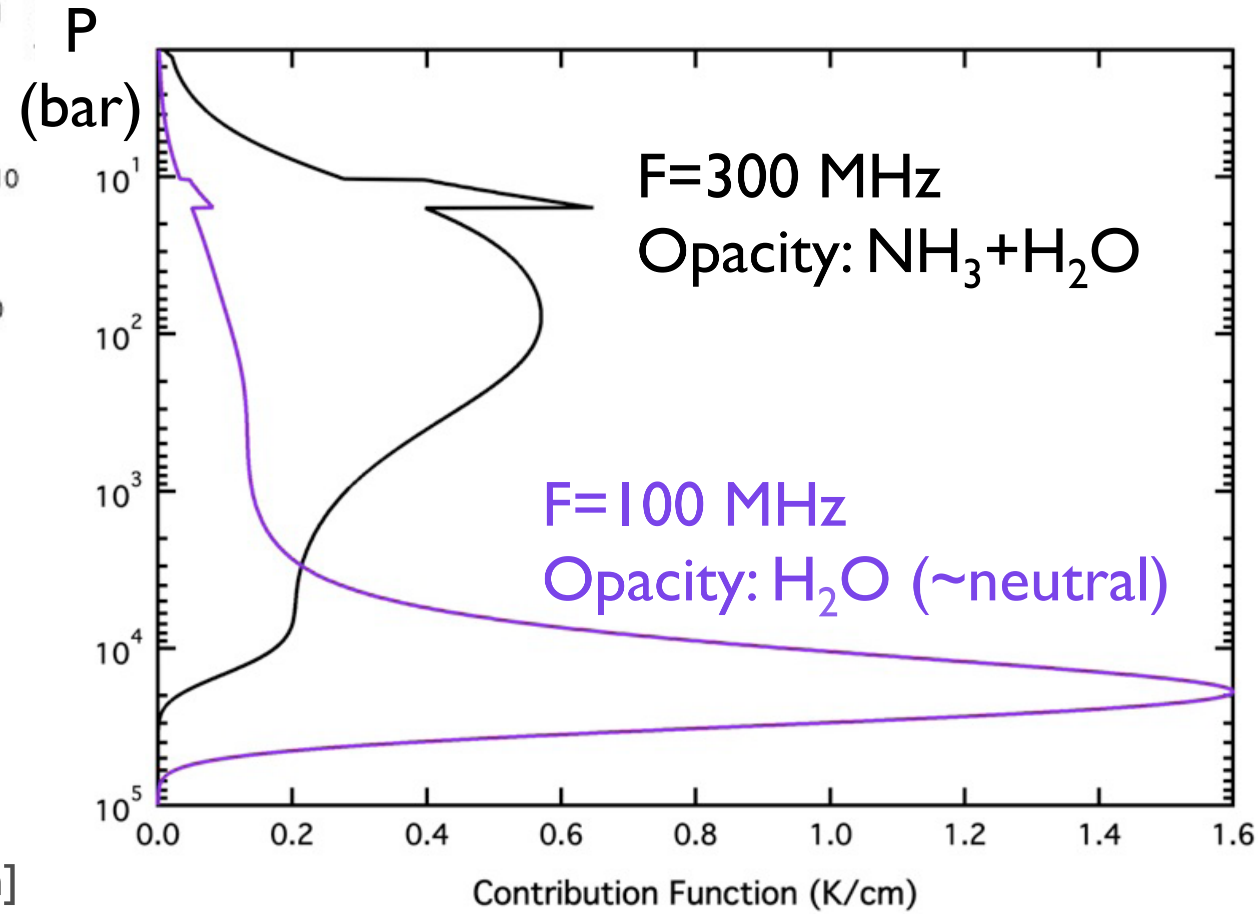

[Priv. com. Hofstadter, Courtin]

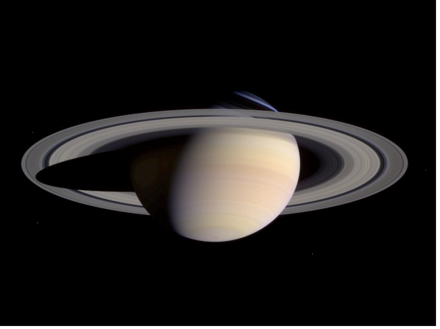

Saturn radiation belts emission

- Lower magnetic field (/10 B_{jup}) & e^- energy (<10 MeV)
- e^- losses due to interaction with the rings / satellites
- Expected flux density: 0.15-0.45 mJy

Extreme Earth/Saturn configurations

→ Detection challenge from the ground

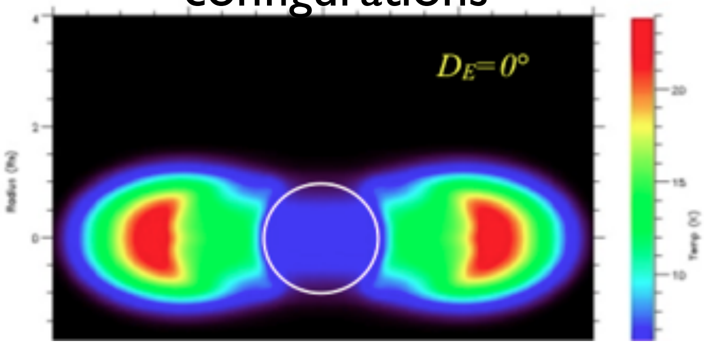

D_E = 0°

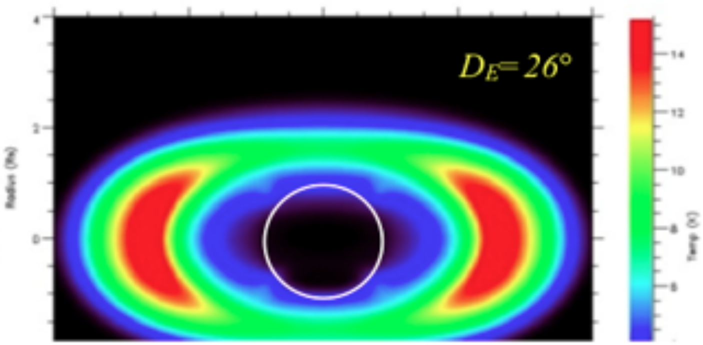

D_E = 26°

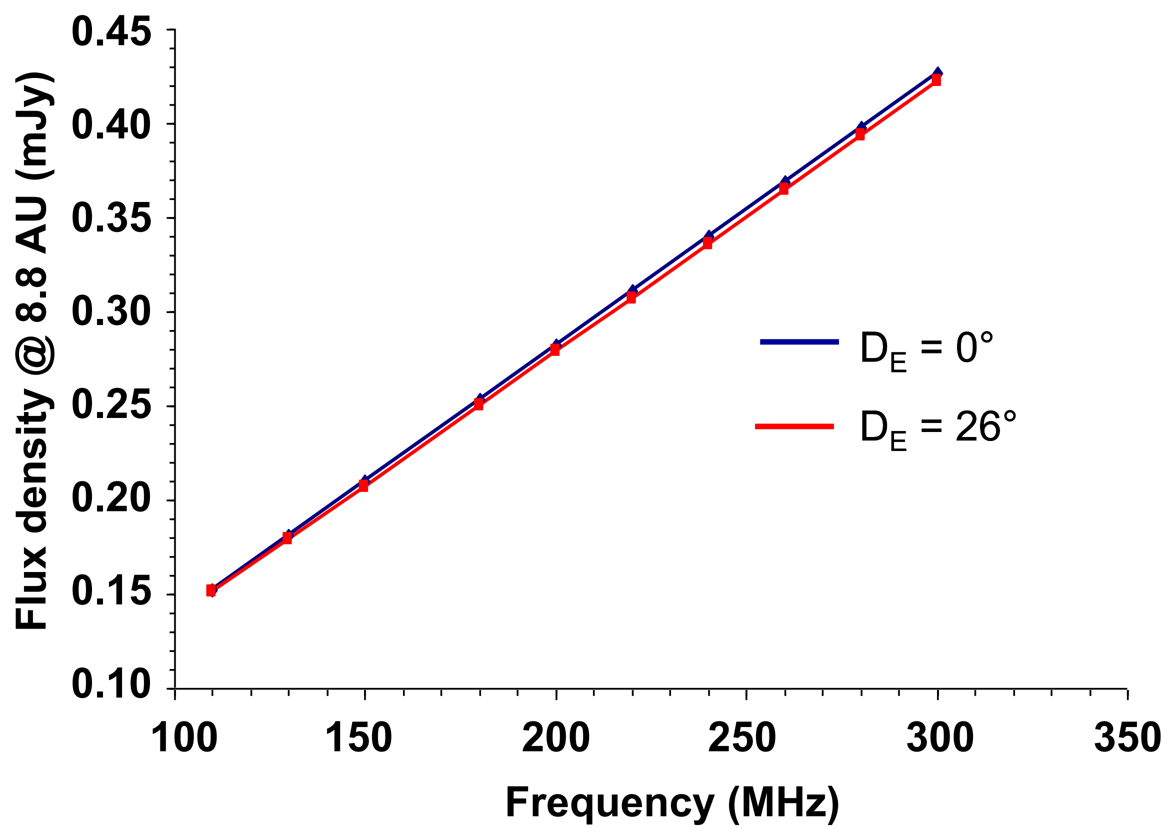

[Lorenzato, 2012, Sicard, 2004, Santos-Costa, 2001]

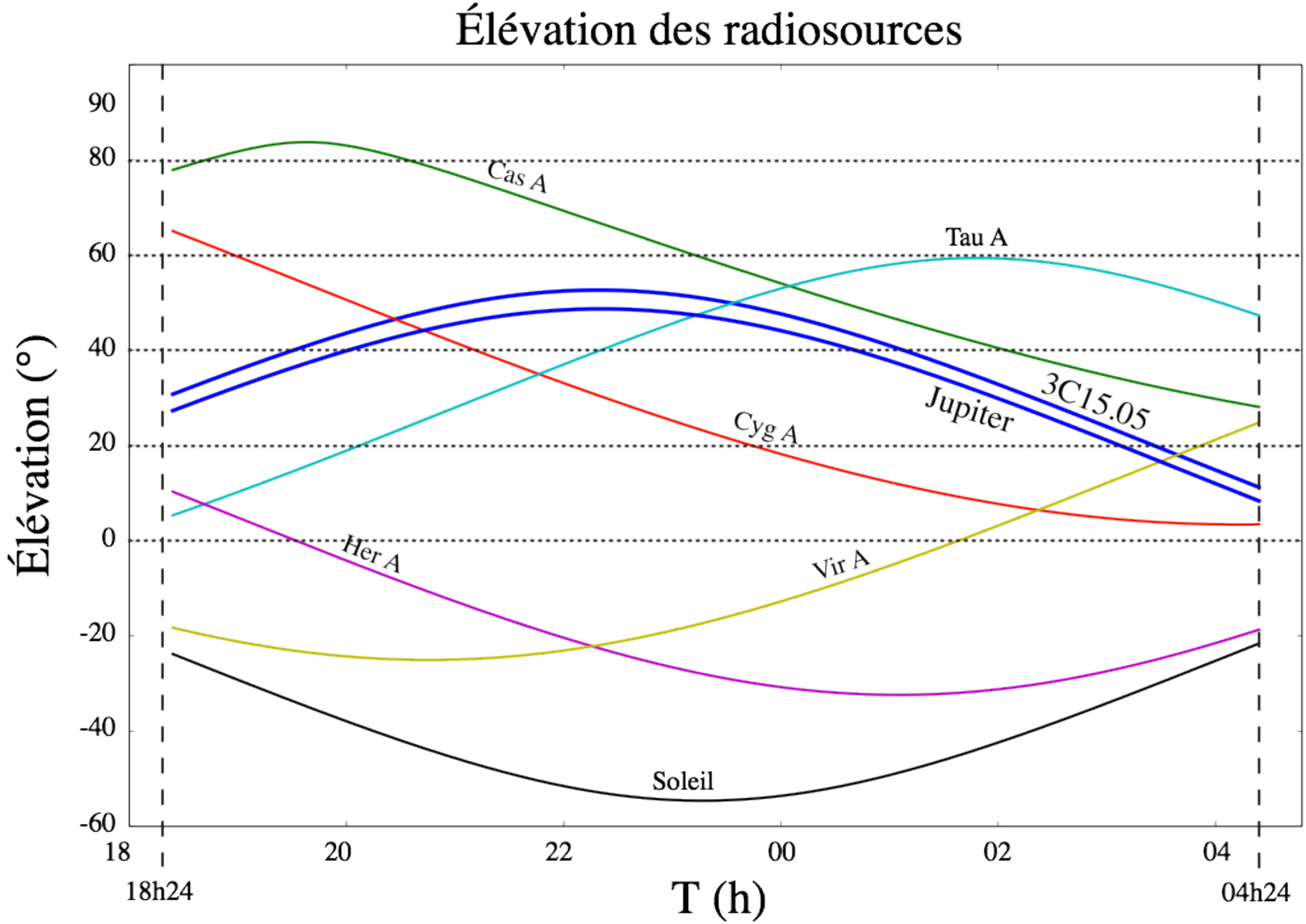
Élévation des radiosources
90
80
60
40
20
0
-20
-40
-60
Élévation (°)
Cas A
Tau A
3C15.05
Jupiter
Cyg A
Her A
Vir A
Soleil
18
20
22
00
02
04
18h24
04h24
T (h)

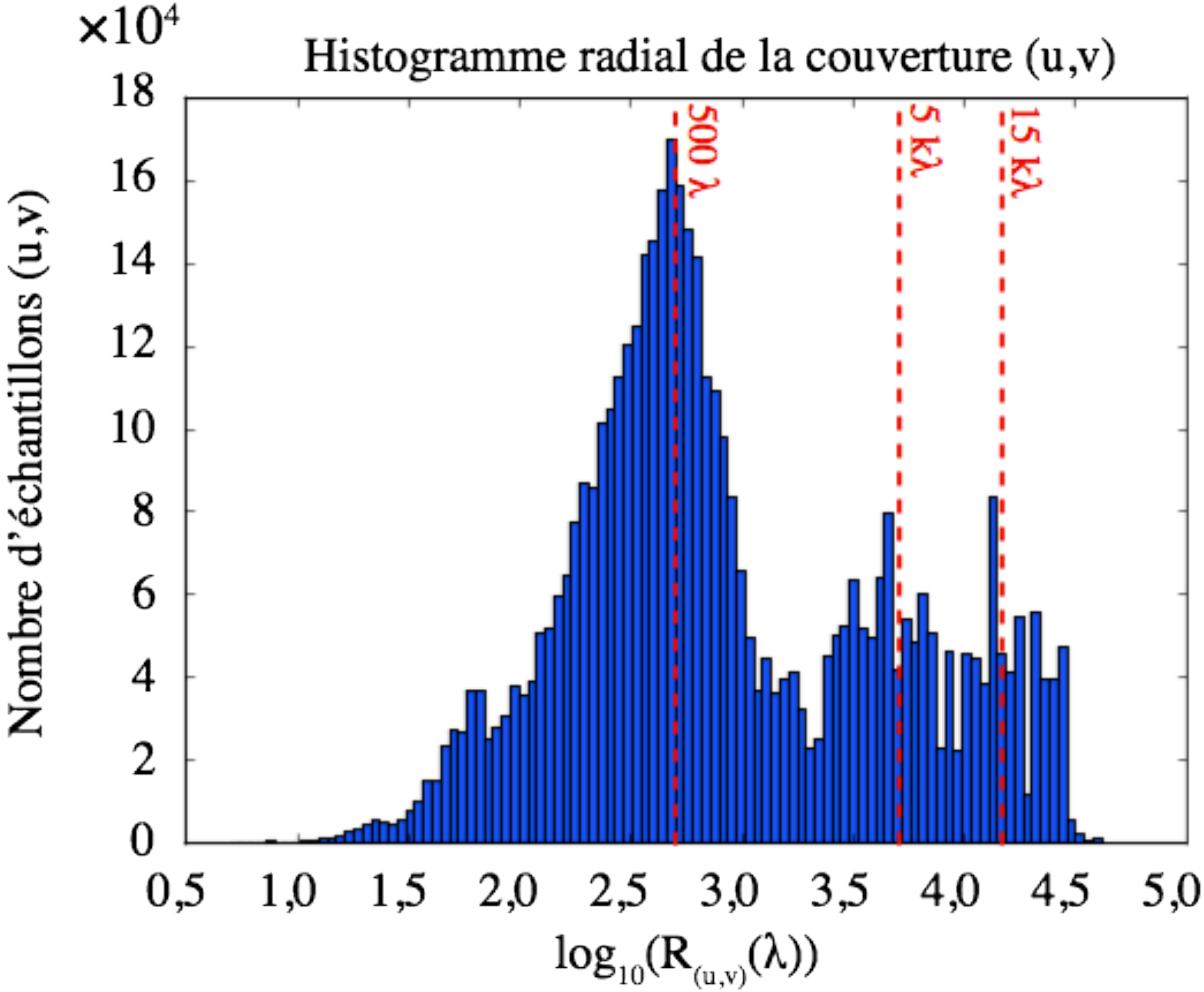
×10^4
Histogramme radial de la couverture (u,v)
Nombre d'échantillons (u,v)
18
16
14
12
10
8
6
4
2
0
500 λ
5 kλ
15 kλ
0,5
1,0
1,5
2,0
2,5
3,0
3,5
4,0
4,5
5,0
log10(R(u,v)(λ))

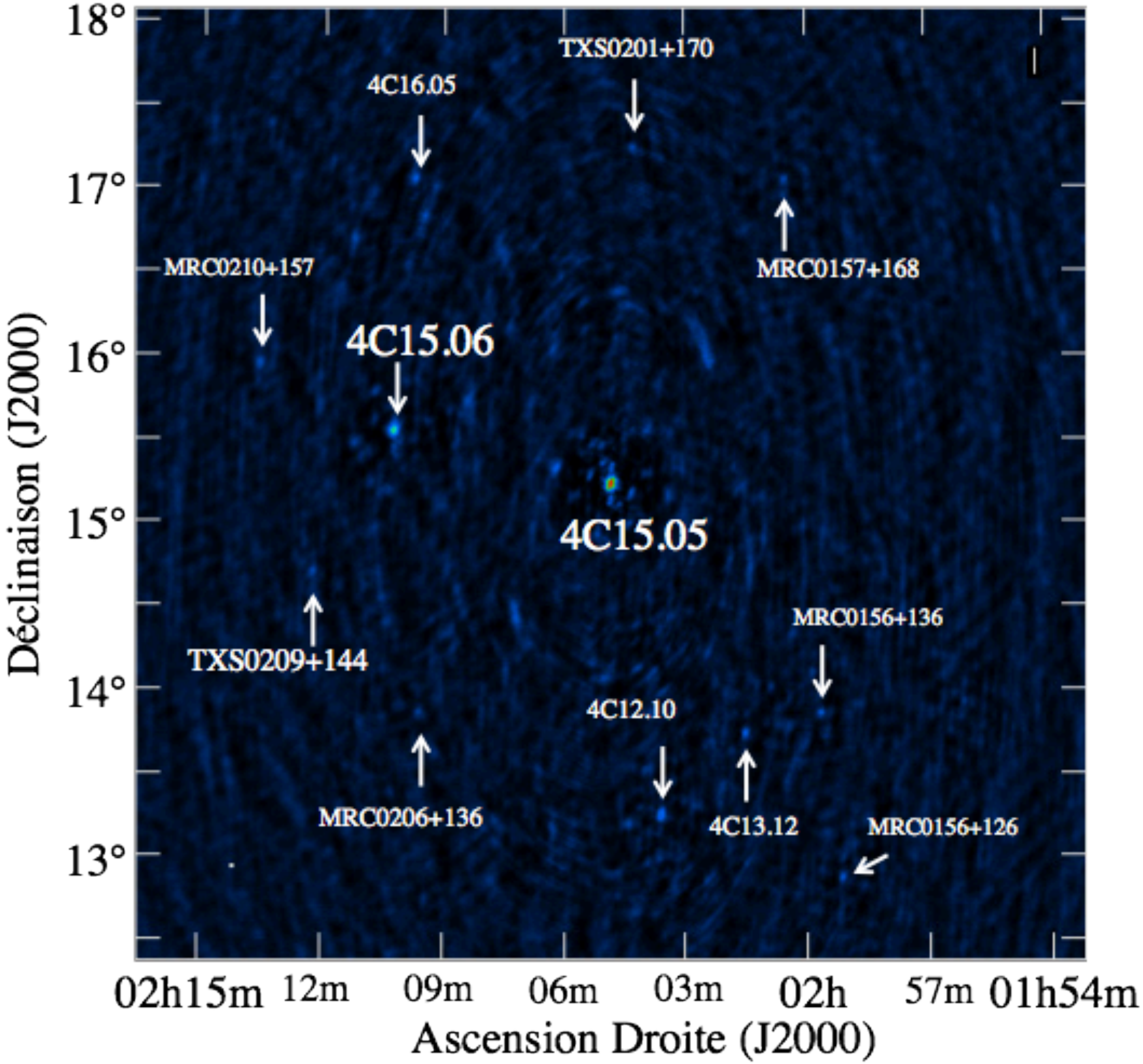
18°
17°
16°
15°
14°
13°
Déclinaison (J2000)
TXS0201+170
4C16.05
MRC0210+157
MRC0157+168
4C15.06
4C15.05
MRC0156+136
TXS0209+144
4C12.10
MRC0206+136
4C13.12
MRC0156+126
02h15m
12m
09m
06m
03m
02h
57m
01h54m
Ascension Droite (J2000)

Spectre des sources voisines

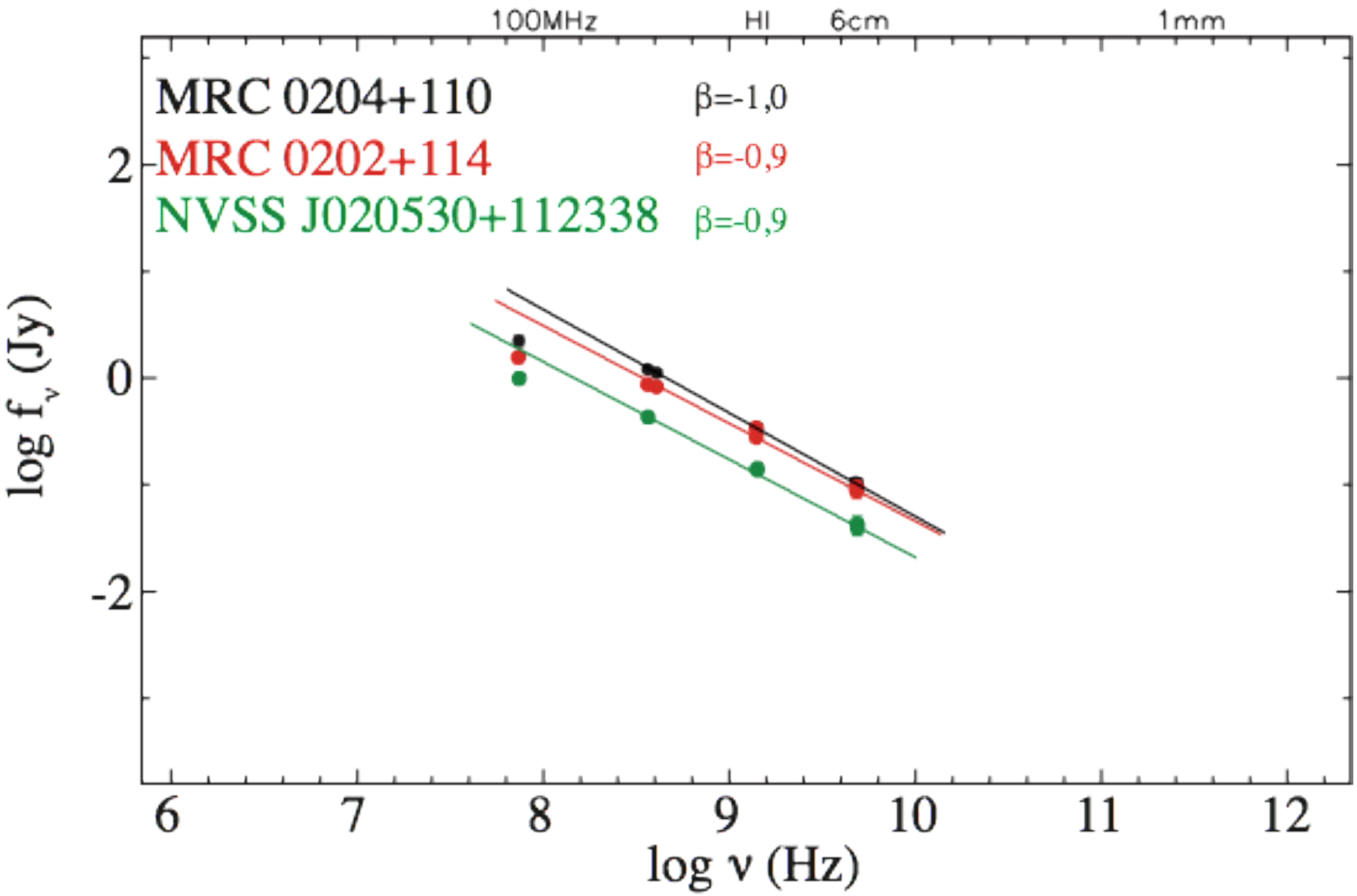

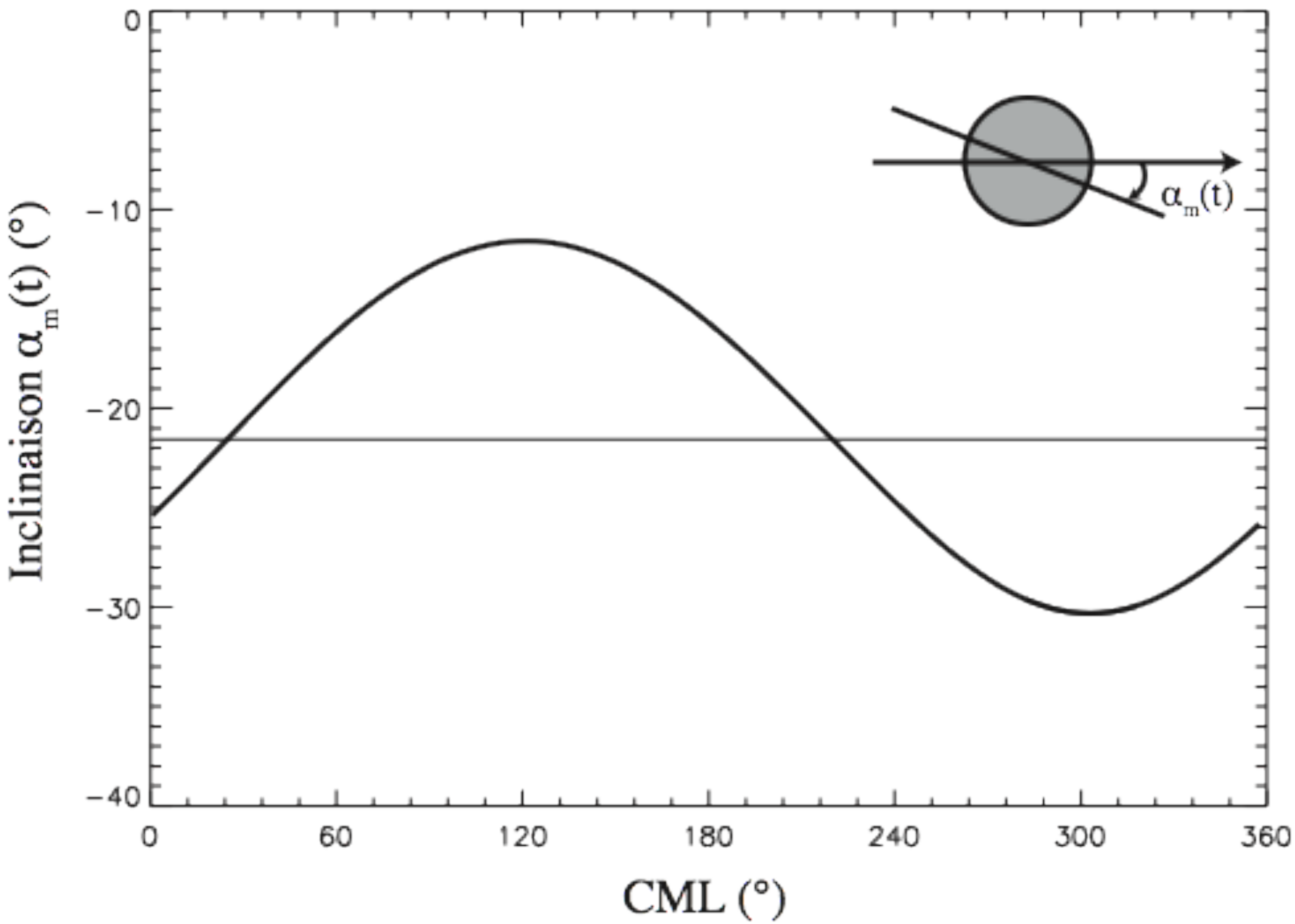

Inclinaison $\alpha_m(t)$ (°)
0
−10
−20
−30
−40
$\alpha_m(t)$
0
60
120
180
240
300
360
CML (°)

Latitude system

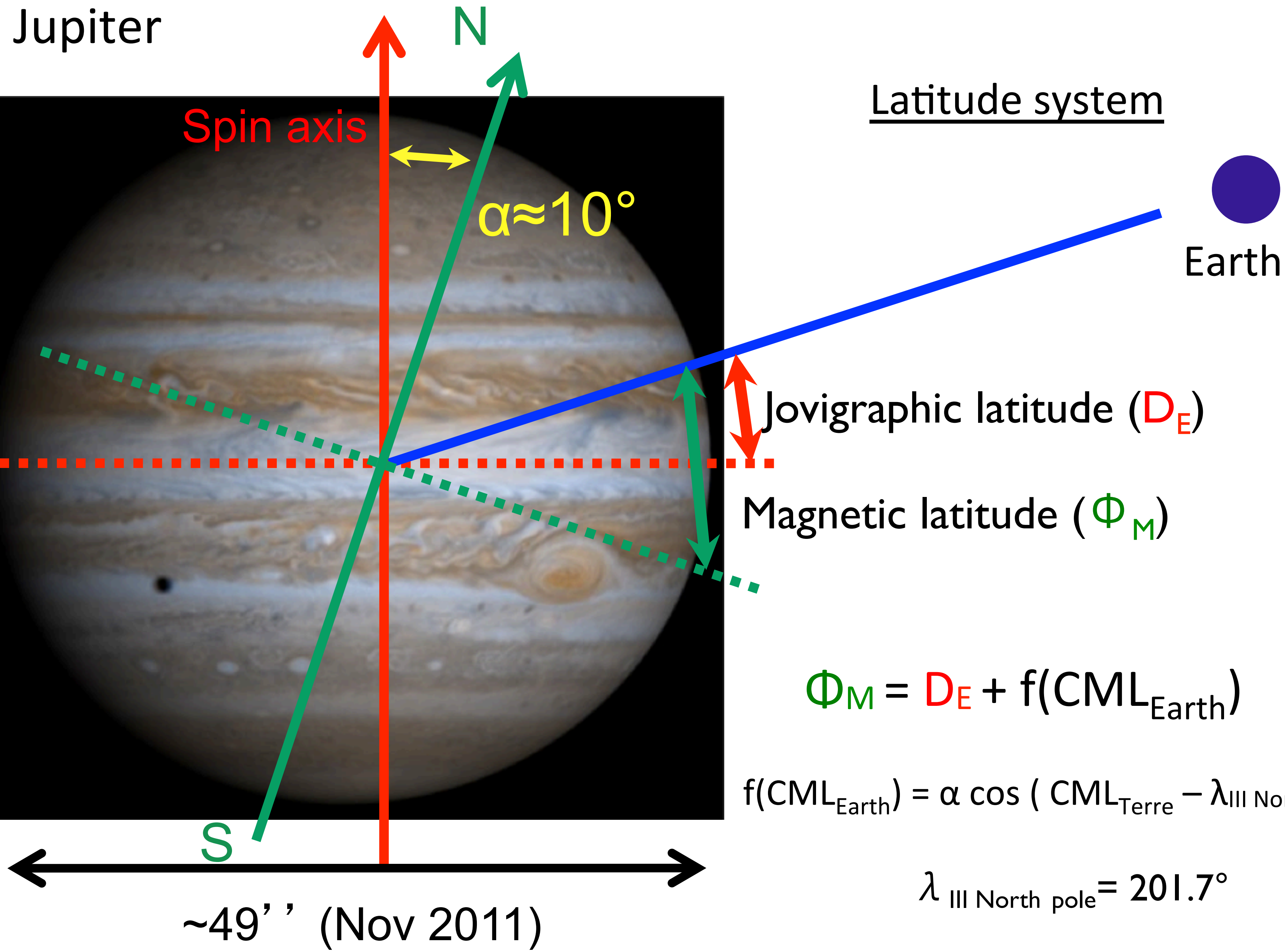

$$\Phi_M = D_E + f(CML_{Earth})$$

$$f(CML_{Earth}) = \alpha \cos\left(CML_{Terre} - \lambda_{III\ North\ pole}\right)$$

$$\lambda_{III\ North\ pole} = 201.7°$$

Jupiter

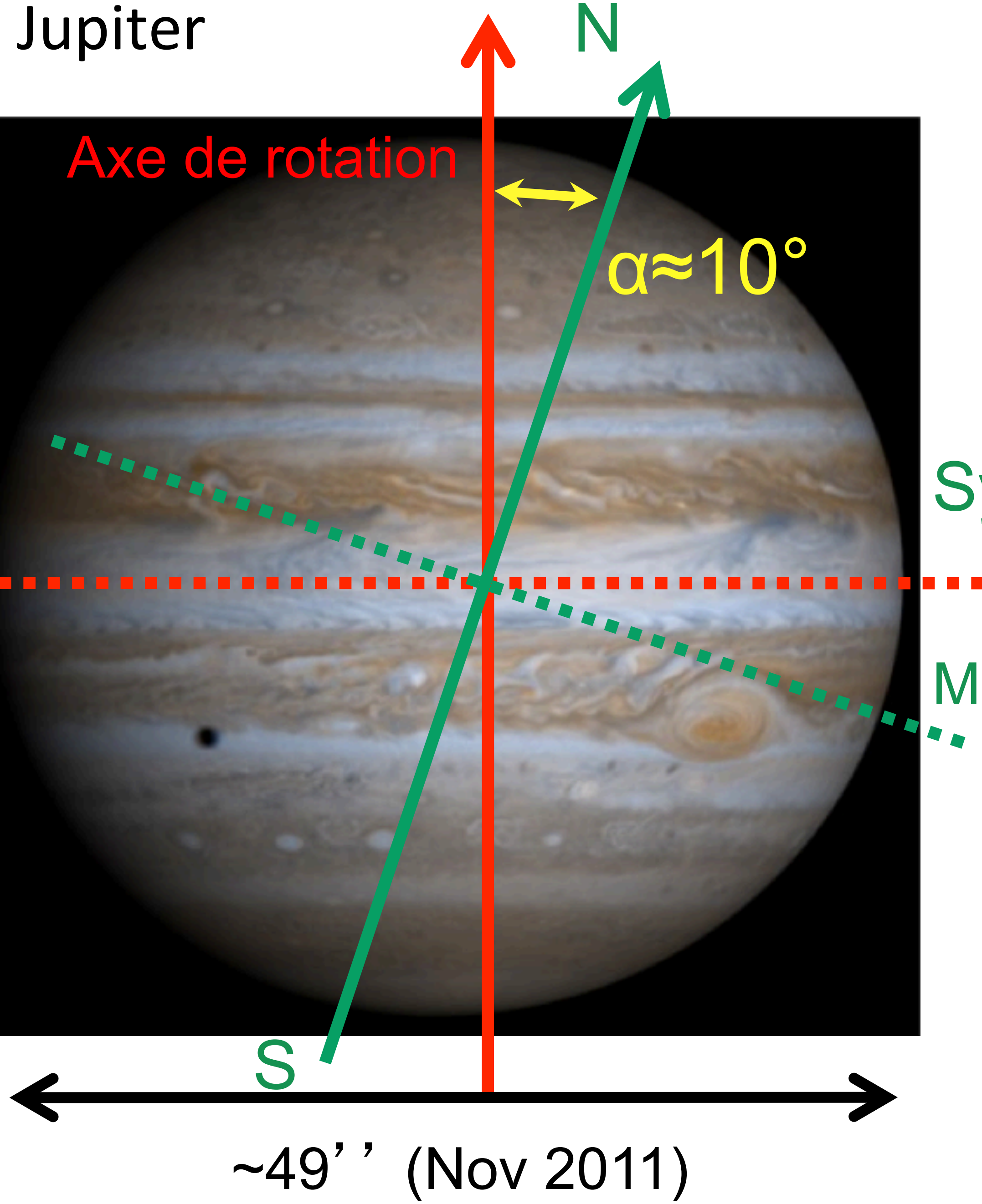

System III (1965)

Dynamic equator

Magnetic equator

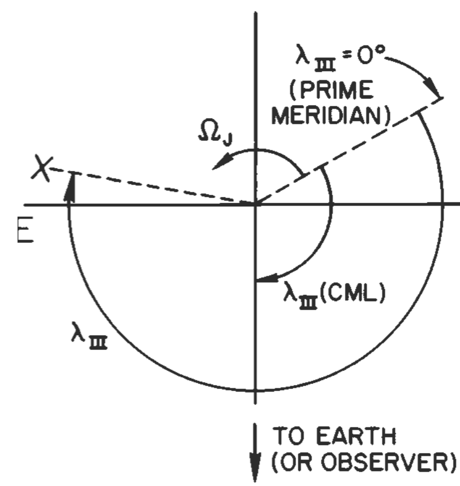

Longitude

λ_{III}

Longitude du méridien central (CML)

Beaming

Émission maximale quand l' observateur passe à l' équateur magnétique

Magnetic Latitude = D_E + 9.6° cos(CML-$\lambda_{III,NP}$)

D_E = jovicentric latitude of Earth = 3.29° in Nov. 2011

[Berge, 1966]

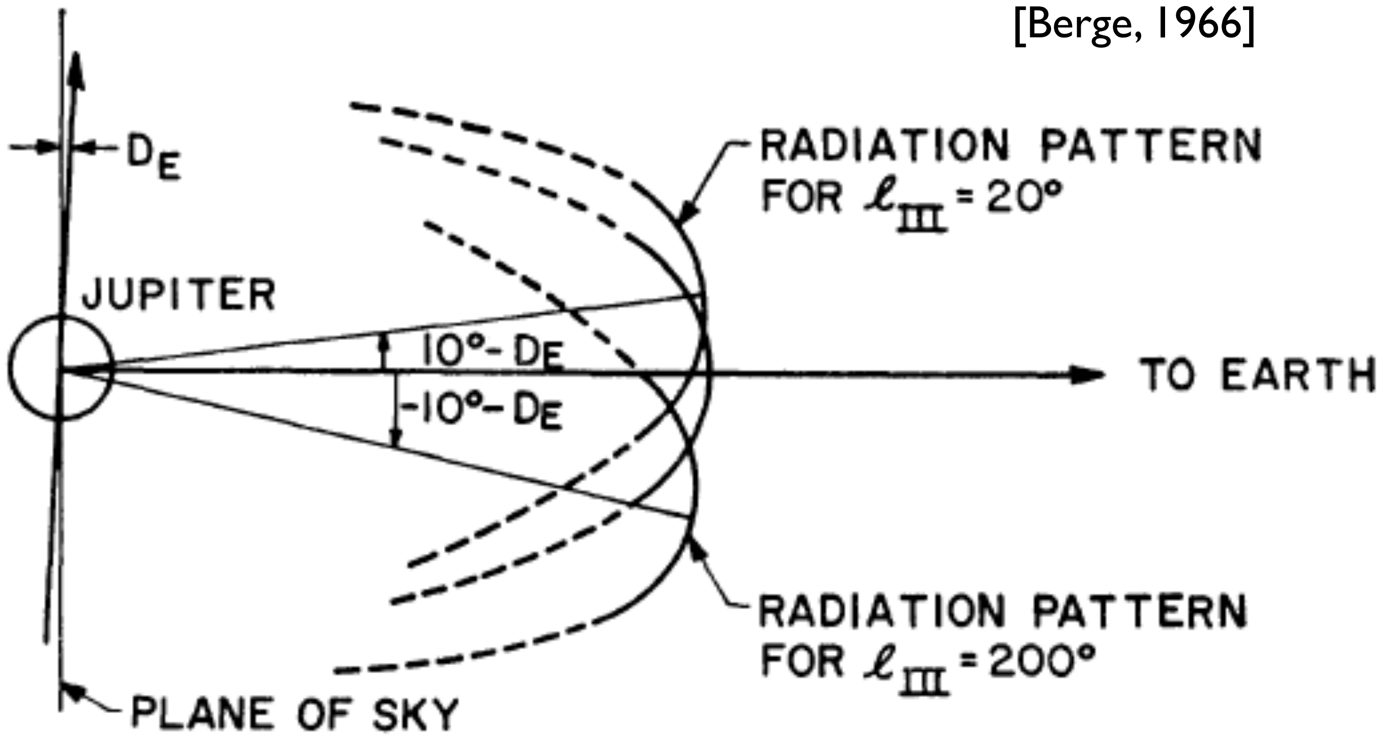

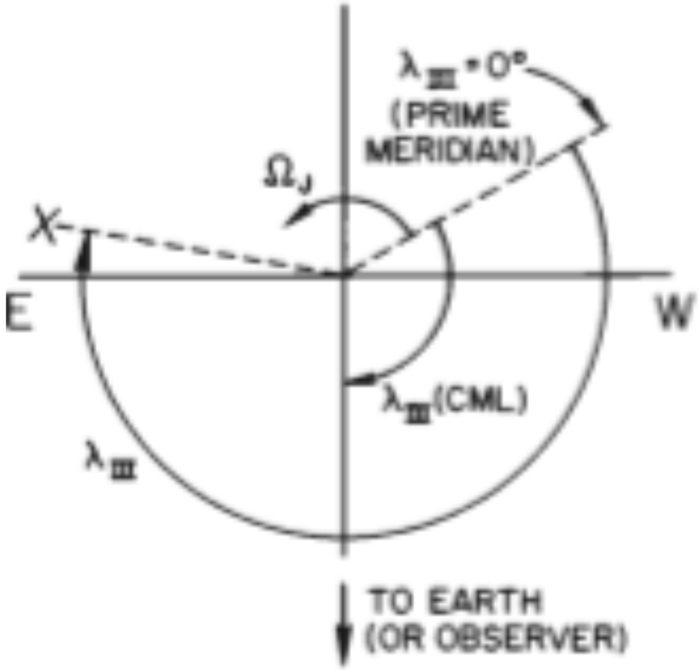
λ_III = 0°
(PRIME
MERIDIAN)
Ω_J
X
E
W
λ_III (CML)
λ_III
TO EARTH
(OR OBSERVER)

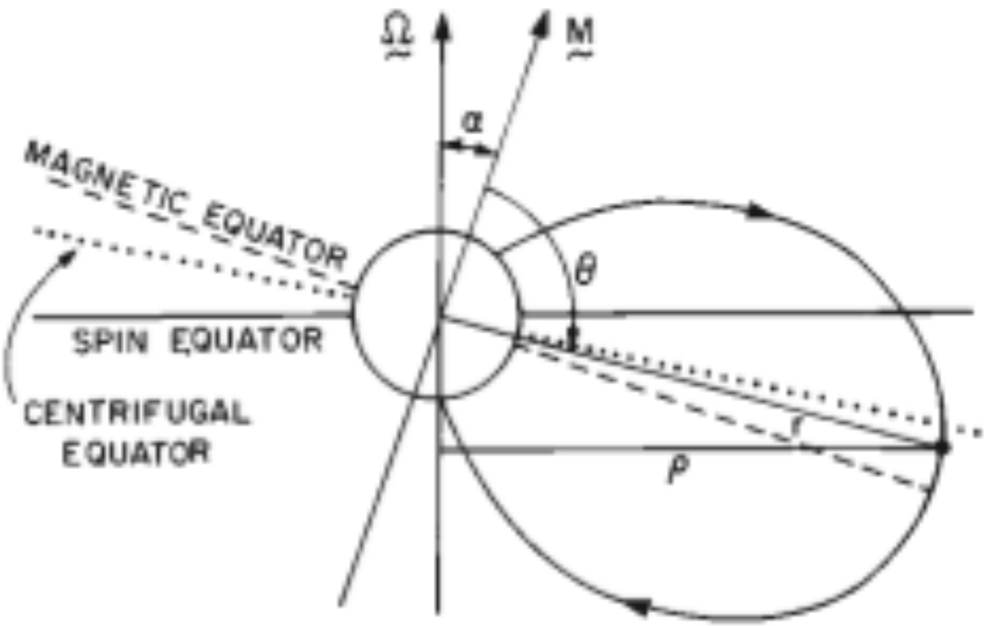
Ω
M
α
MAGNETIC EQUATOR
θ
SPIN EQUATOR
CENTRIFUGAL
EQUATOR
r
ρ

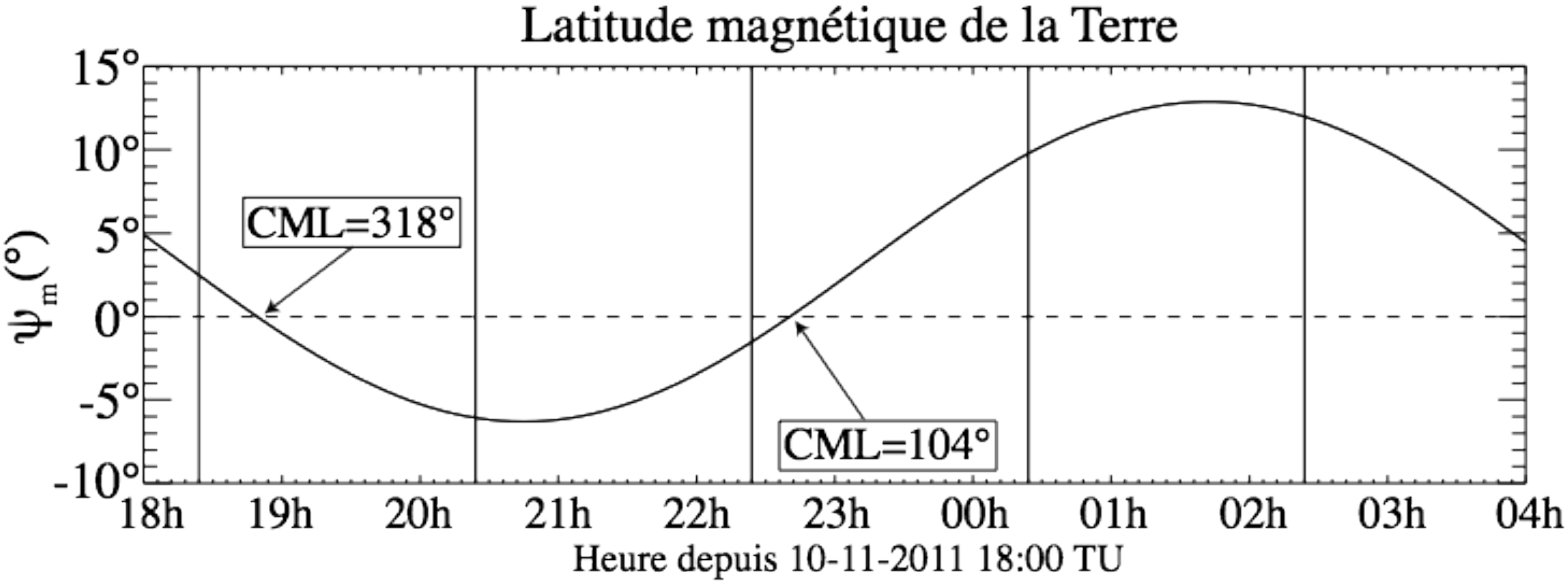
Latitude magnétique de la Terre
15°
10°
5°
0°
-5°
-10°
ψ_m(°)
CML=318°
CML=104°
18h
19h
20h
21h
22h
23h
00h
01h
02h
03h
04h
Heure depuis 10-11-2011 18:00 TU

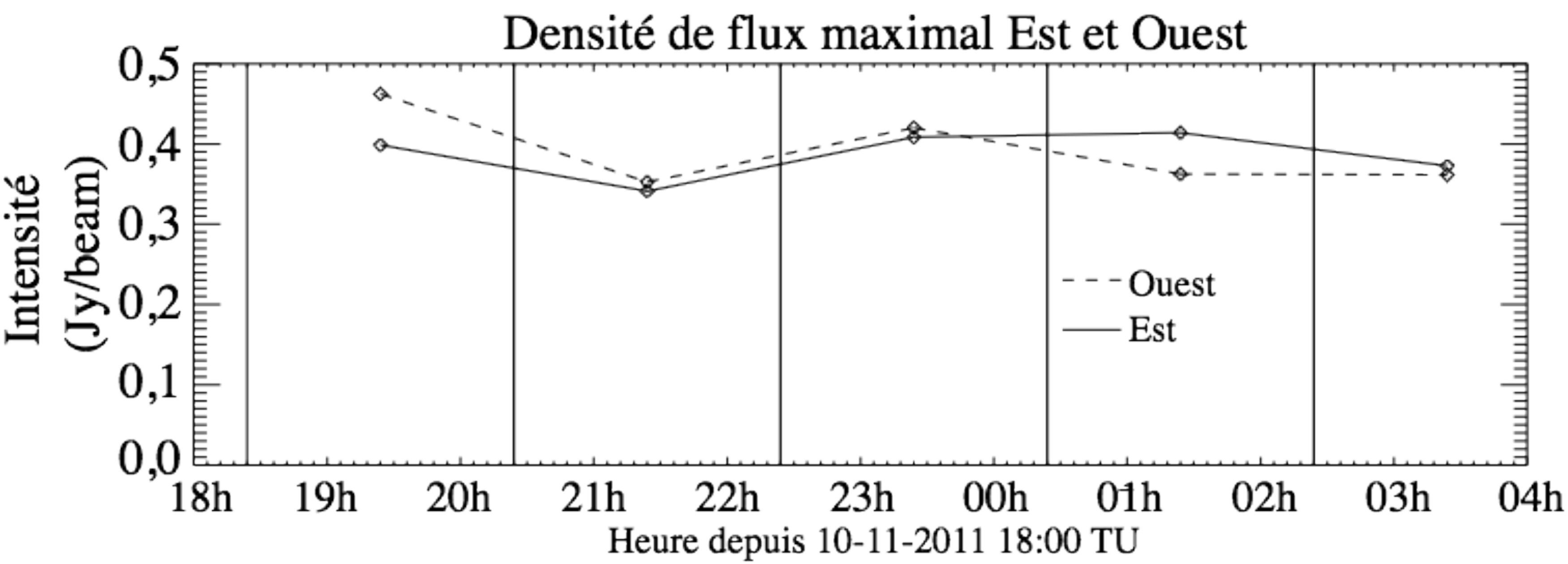
Densité de flux maximal Est et Ouest
0,5
0,4
0,3
0,2
0,1
0,0
Intensité
(Jy/beam)
Ouest
Est
18h
19h
20h
21h
22h
23h
00h
01h
02h
03h
04h
Heure depuis 10-11-2011 18:00 TU

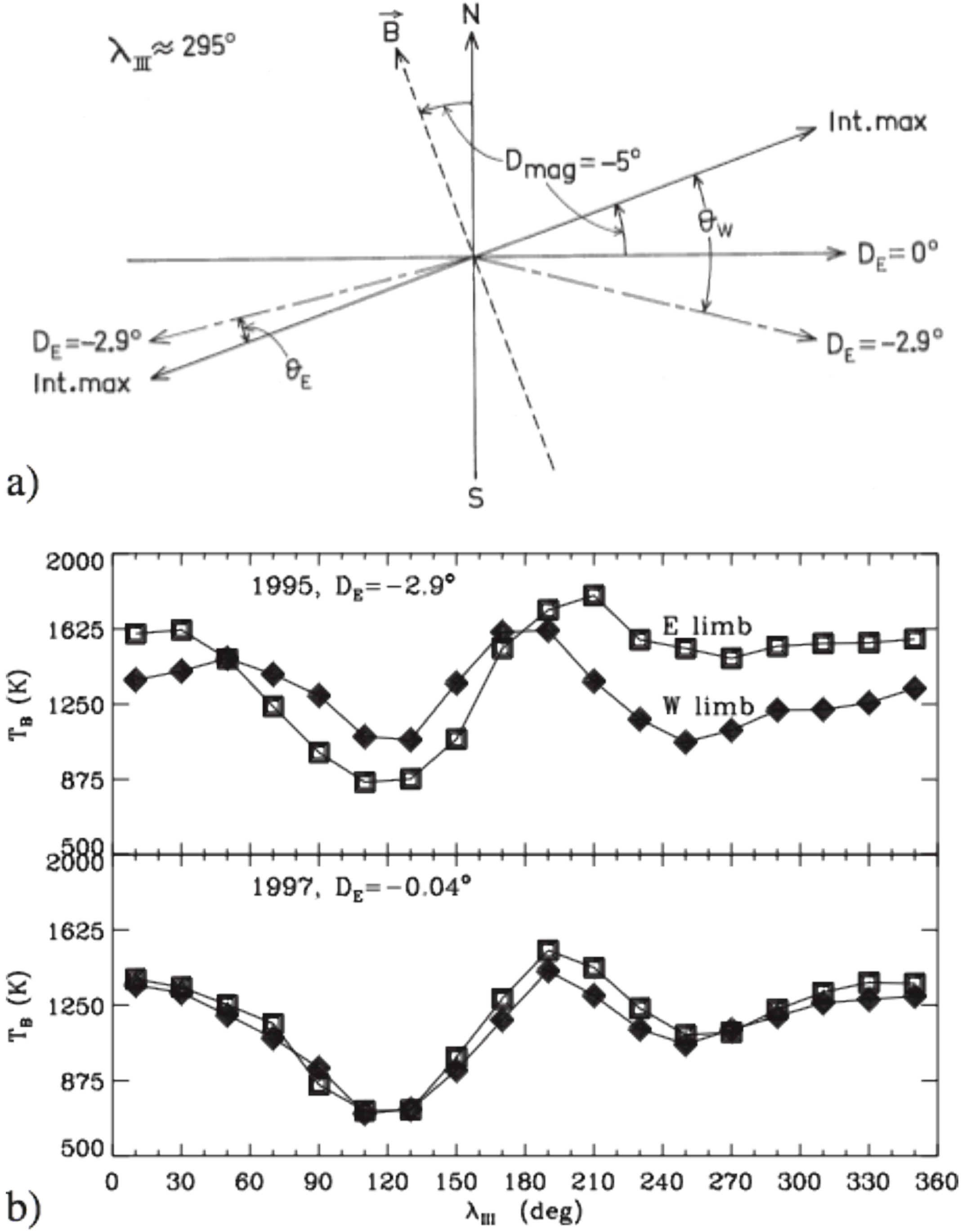

λ_III ≈ 295°
B
N
Int.max
D_mag = -5°
θ_W
D_E = 0°
D_E = -2.9°
Int.max
θ_E
D_E = -2.9°
S
a)
1995, D_E = -2.9°
E limb
W limb
T_B (K)
2000
1625
1250
875
500
1997, D_E = -0.04°
0
30
60
90
120
150
180
210
240
270
300
330
360
λ_III (deg)
b)

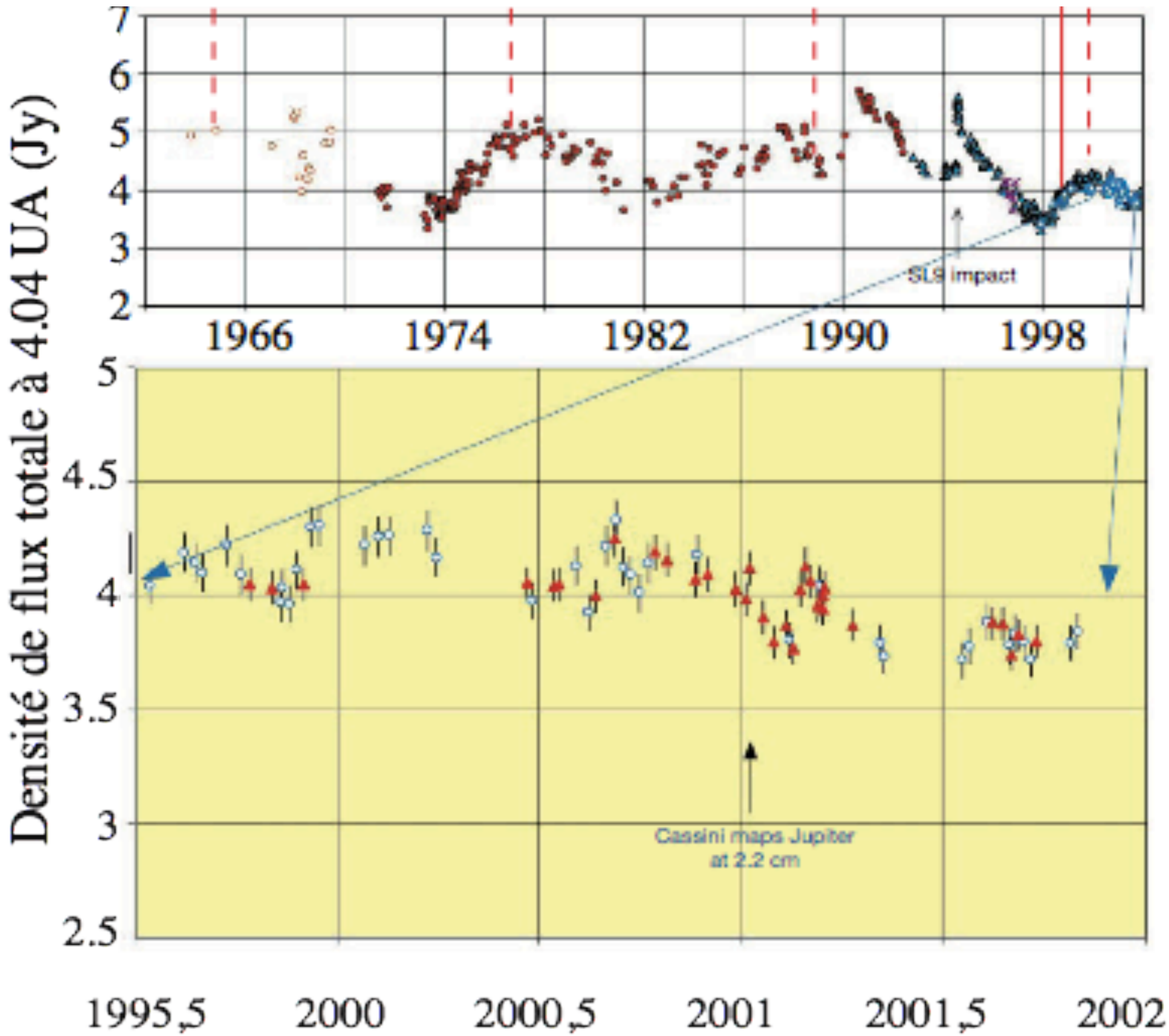

Densité de flux totale à 4.04 UA (Jy)
7
6
5
4
3
2
1966
1974
1982
1990
1998
SL9 impact
5
4.5
4
3.5
3
2.5
Cassini maps Jupiter at 2.2 cm
1995,5
2000
2000,5
2001
2001,5
2002

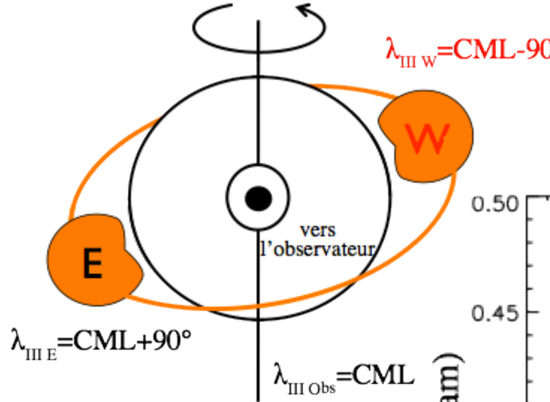
λIII W=CML-90
W
E
vers l'observateur
λIII E=CML+90°
λIII Obs=CML

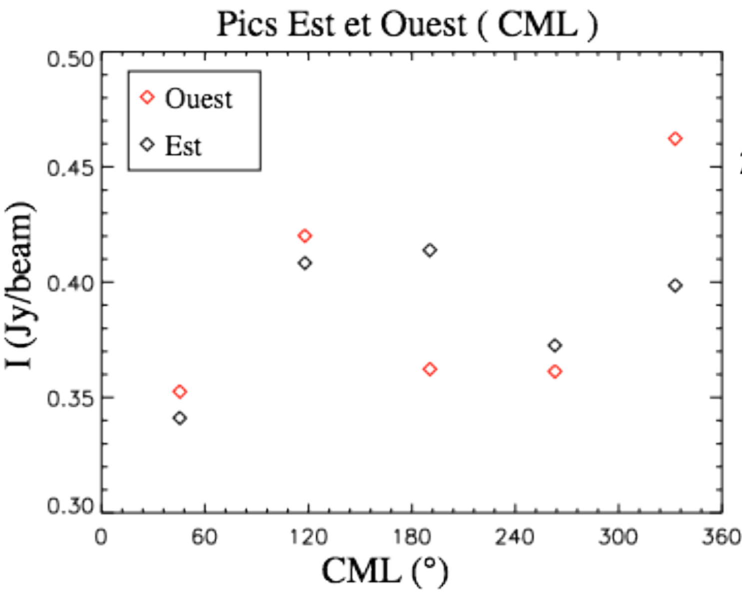
Pics Est et Ouest (CML)
Ouest
Est
I (Jy/beam)
CML (°)
0.30
0.35
0.40
0.45
0.50
0
60
120
180
240
300
360

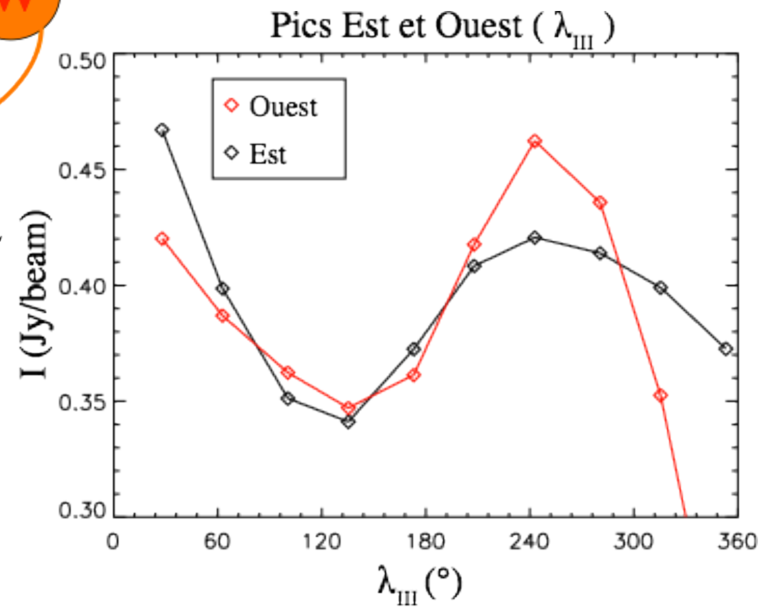
Pics Est et Ouest (λIII)
Ouest
Est
I (Jy/beam)
λIII (°)
0.30
0.35
0.40
0.45
0.50
0
60
120
180
240
300
360

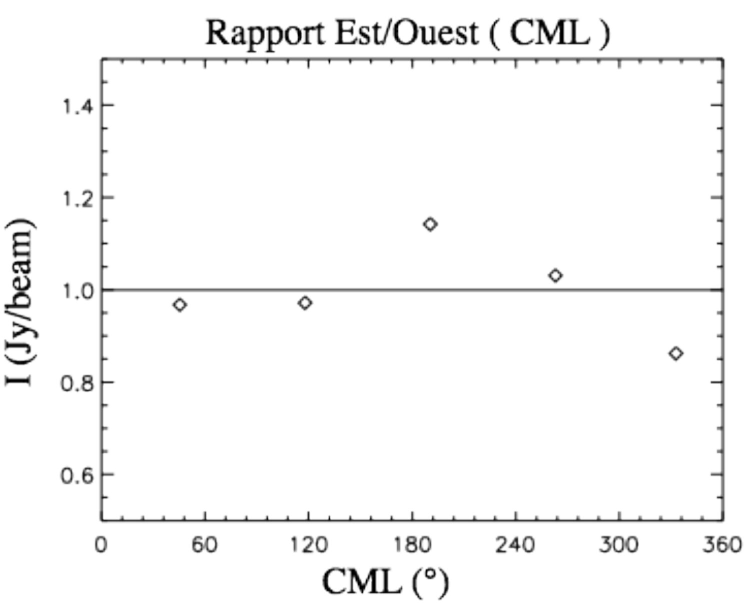
Rapport Est/Ouest (CML)
I (Jy/beam)
CML (°)
0.6
0.8
1.0
1.2
1.4
0
60
120
180
240
300
360

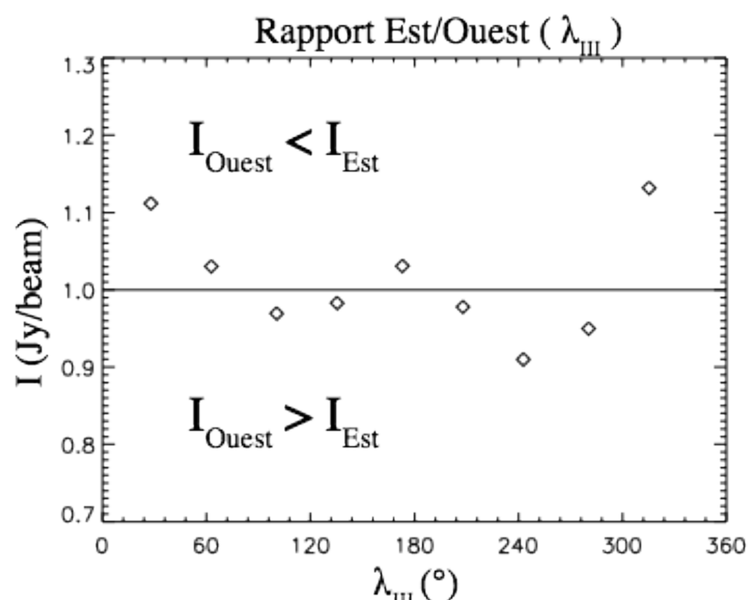
Rapport Est/Ouest (λIII)
IOuest < IEst
IOuest > IEst
I (Jy/beam)
λIII (°)
0.7
0.8
0.9
1.0
1.1
1.2
1.3
0
60
120
180
240
300
360

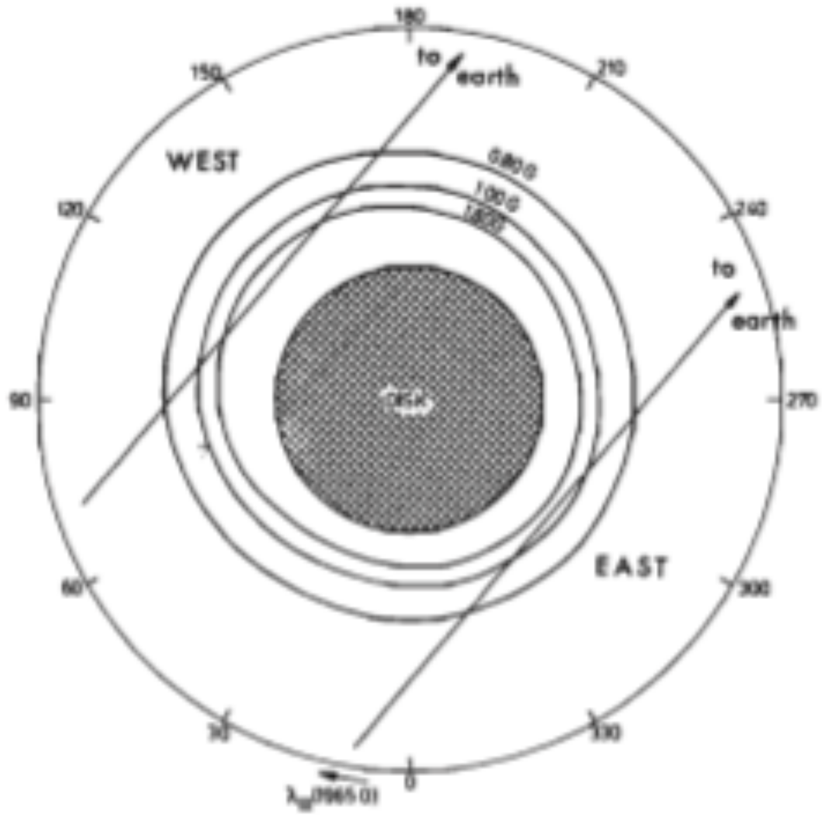

Fig. 8. View on top of Jupiter with three B - const contours of 1.80, 2.00, and 0.80 G in the magnetic equatorial surface of the O_4 model and two lines of sight to the observer at equal distances from the planet, for a central meridian longitude of 220°.

a

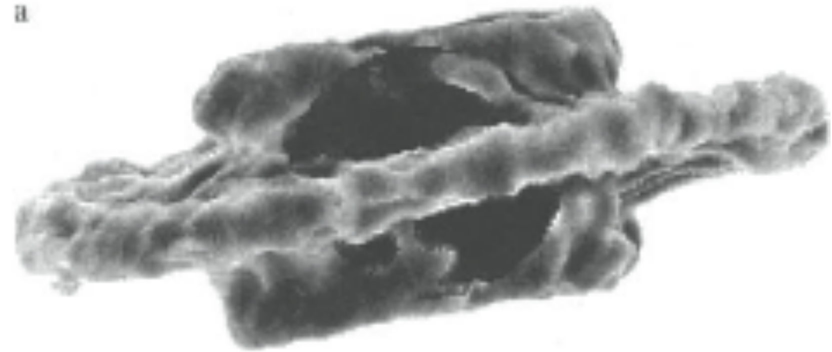

b